Buckling of a compliant hollow cylinder attached to a rotating rigid shaft

Serge Mora, Franck Richard

Buckling of a compliant hollow cylinder attached to a rotating rigid shaft

Serge Mora* and Franck Richard

Laboratoire de Mécanique et de Génie Civil,

Université de Montpellier and CNRS.

163 rue Auguste Broussonnet. F-34090 Montpellier, France.

(Dated: April 18, 2019)

Abstract

Bifurcations in the equilibrium shape of a thick elastic layer attached to a circular rigid cylinder rotating about its axis are investigated analytically and numerically. The centrifugal force breaks the symmetry of the system leading to deformations invariant along the axis as the result of an instability. The instability threshold depends at linear order on the relative thickness of the compliant layer, and on a dimensionless control parameter based on the elastic modulus, the angular velocity and the outer radius. A weakly non linear analysis, carried out for layers following the Mooney-Rivlin constitutive law, points out the discontinuous (sub-critical) features of the bifurcation, except for relative thickness laying in a very narrow range in which the bifurcation is super-critical. Numerical simulations in the fully post-buckled regime yield the absolute instability threshold, and the order in the rotational symmetry of the developed equilibrium shape.

PACS numbers: 46.32.+x,46.25.-y,47.20.Ma,83.80.Kn

*serge.mora@umontpellier.fr

I. INTRODUCTION

Slender pieces can rotate at high angular velocity in mechanical devices such as ultra-centrifuges, spin-coaters, or high-speed thermal engines. These pieces, made of rigid material such as metal or composite, are usually cylindrical to avoid unbalance. Connecting pieces between these rotating rods are often used. For instance, thermal insulators or expansion joints are placed at the junction between two shafts. In addition, insulators (thermal or electrical) can cover the rigid shaft to protect it from external disturbances as a sudden increase of the outer temperature or an unexpected electrical current. These insulators are often polymer-based materials which are much more compliant than the central shaft. The study of the mechanical behavior of the system consisting in a rigid right circular cylinder surrounded by a hollow cylinder made in a flexible elastic material, subjected to high angular velocities, is therefore an important issue for advanced applications.

Spinning cylinders coated with elastic layers also provides a new route for (micro)patterning, like designing periodic longitudinal grooves of controlled depth and wavelength at the surface of cylinders: as shown below, the periodic shape appearing spontaneously at the outer surface can be controlled by adjusting the layer thickness and the angular velocity (after that, the pattern can be fixed by initiating a chemical reaction).

Following the pioneering works of Patterson, Haughton and Ogden, and Rabier and Oden [1–3], bifurcations in the equilibrium shape of *homogeneous* elastic (solid) cylinders rotating about their own axis were investigated in a previous article [4], by considering the limit of infinitely thin central inner rigid rods. At the linear order in terms of the amplitude of the deformations, these bifurcations were described with a unique dimensionless control parameter $\alpha = \rho r_0^2 \omega^2 / \mu$, with ρ the mass density of the elastic material, μ the shear modulus, r_0 the radius and ω the angular velocity. The linear analysis evidenced an instability threshold at $\alpha = 3$, leading to a prismatic deformation of the cylinder (the deformation is invariant under any translation along the axis) consisting in an ovalization of the cross section with a rotational symmetry of order 2. The details of the constitutive law of the elastic material were found to be crucial in order to properly describe the nature of the bifurcation (super-critical or sub-critical) as well as the amplitude of the deformation and the moment of inertia as a function of the control parameter. It has also been shown that for any constitutive law, the main features of the bifurcation can be deduced from the instability of a neo-Hookean elastic cylinder with an apparent shear modulus [4].

Here we consider the more common structure consisting in rigid shafts of finite radius, concentrically coated with a compliant material, spinning in air about their axis. We first investigate the linear stability of the elastic cylindrical shell (Sec. III). It is first unstable against a prismatic deformation beyond a critical angular velocity ω_c. ω_c depends on the relative thickness of the layer, on the outer radius, the shear modulus of the compliant layer and its mass density. Then a weakly non linear analysis addresses the nature of the bifurcation. We demonstrate that depending on the relative thickness of the elastic layer the transition can be super-critical or sub-critical (Sec. IV). Finally numerical simulations address the post-buckled regime (Sec. V).

II. EQUILIBRIUM CONDITION

A rigid rod with a circular cross section of radius ar_0 $(0 < a < 1)$ is surrounded by an elastic isotropic and incompressible material of thickness $(1-a)r_0$ with the mass density ρ and the shear modulus μ. The cylindrical elastic layer is attached to the rigid rod. The whole system is subjected to the angular velocity ω around the axis (Fig.1).

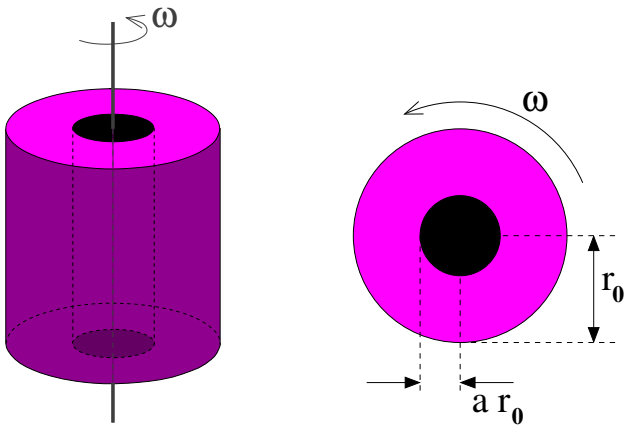

FIG. 1: A cylindrical shell made of an elastic, isotropic and incompressible material is attached to a rigid rod. The outer radius of the cylindrical shell is r_0, the inner radius is ar_0. The whole system is rotating with angular velocity ω about the z-axis.

We work in the frame rotating with the cylinder, and seek equilibrium (*i.e.* static) solutions in the presence of centrifugal forces. The constant angular velocity is assumed to be switched on a long time ago, so that the system has reached its equilibrium configuration and transients and

other dynamic effects are ignored (transient regimes are assumed to be damped by the dissipative processes). As a result, this problem is fundamentally different from the classical problem of 'standing waves' in tires, which develop when the vehicle reaches a critical velocity; such waves appear as stationary to an observer moving with the vehicle (hence the somewhat improper name of 'standing waves') but are *not* stationary in a frame co-rotating with the tire [5–8]. The symmetry is broken by the 'moving' contact forces with the road and not by an instability. In the presence of viscoelasticity or any other sources of dissipation, the moving contact forces supply energy continuously into the system, and no 'standing waves' can appear if the contact forces are removed [9]. By contrast, the elastic bifurcation we study in this paper can take place even in the presence of viscoelastic dissipation [10], as spinning motion is a rigid-body rotation, even after a bifurcation has taken place.

In the rotating frame we consider, the equilibrium shape results from the competition between the elastic force and the centrifugal force, two conservative forces. The static mechanical equilibrium is established in a configuration in which the gradient of the potential energy with respect to the deformation is zero. The deformation of the compliant cylindrical layer is characterized by a map from the position $\mathbf{r}$ of the material in the unbuckled configuration to the spatial position $\mathbf{R}(\mathbf{r})$ in the deformed configuration. For an isotropic and incompressible elastic material, the density of elastic energy depends on the two first invariants, I_1 and I_2, of the Green's deformation tensor defined as $\mathbf{C} = \mathbf{F}^T.\mathbf{F}$, where $\mathbf{F}$ is the deformation gradient (formally, $\mathbf{F} = \partial\mathbf{R}/\partial\mathbf{r}$): $I_1 = \mathrm{tr}\ \mathbf{C}$ and $I_2 = \frac{1}{2}\left((\mathrm{tr}\ \mathbf{C})^2 - \mathrm{tr}\ (\mathbf{C}^2)\right)$. The elastic energy density can be written as $\mu W(I_1, I_2)$ where W is a dimensionless function depending on the non linear features of the material. μ being the shear modulus, the dimensionless elastic energy density has to fulfill the condition:

$$\frac{\partial W}{\partial I_1}(0,0) + \frac{\partial W}{\partial I_2}(0,0) = \frac{1}{2}. \tag{1}$$

Incompressibility is imposed by writing that the determinant J of $\mathbf{F}$ is equal to one. In order to characterize equilibrium configurations, the quantity to be minimized with respect to small variations of the displacement is:

$$\mathcal{E} = \int_{ar_0<r<r_0;\ 0<z<h} \mathrm{d}\mathbf{r} \left(\mu W(I_1, I_2) - \frac{1}{2}\rho\omega^2 \left(\mathbf{R}\cdot\mathbf{R} - (\mathbf{R}\cdot\mathbf{e}_z)^2 \right) + \mu q(J-1) \right). \tag{2}$$

The first term in the integral is for the strain energy. The second one is for the potential of the centrifugal force. In the variation, the incompressibility condition, $J = 1$, is enforced everywhere by means of the Lagrange multiplier $q(\mathbf{r})$.

We consider slender cylinders ($h \gg r_0$) and we focus on the area far from the ends of the cylinders, *i.e.* at distances from the cylinder ends significantly larger than r_0. Within this hypothesis, for a fixed value of a and for a given energy density function, the equilibrium of the system is driven by the unique control parameter

$$\alpha = \frac{\rho r_0^2 \omega^2}{\mu}. \tag{3}$$

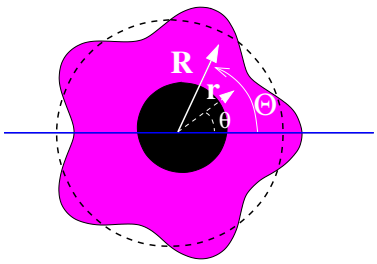

FIG. 2: A material point at radial distance r, polar angle θ and height z in the base (unbuckled) state is displaced, in the deformed state, so that the new radial distance becomes $R(r, \theta, z)$, the polar angle becomes $\Theta(r, \theta, z)$ and the height $Z(r, \theta, z)$.

In the following we use cylindrical coordinates, with r the distance to the axis, θ the angle and z the height in the unperturbed state (Fig.2). After deformation, the polar coordinates become $R(r, \theta, z)$, $\Theta(r, \theta, z)$, and $Z(r, \theta, z)$. The equilibrium equations are derived from the condition that the first variation of Eq.2 with respect to $R(r, \theta, z)$, $\Theta(r, \theta, z)$, $Z(r, \theta, z)$ and $q(r, \theta, z)$ is zero. Let $\mathbf{t} = (R, \Theta, Z, q)$ denote the collection of unknowns, and $\delta\mathbf{t} = (\delta R, \delta\Theta, \delta Z, \delta q)$ a virtual displacement that is kinematically admissible (abbreviated as 'k.a.'), *i.e.* such that $\delta R(ar_0, \theta, z) = 0$, $\delta\Theta(ar_0, \theta, z) = 0$, $\delta Z(ar_0, \theta, z) = 0$ as imposed by the central rigid core. The field $\mathbf{t}(r, \theta, z)$ is a solution of the problem if it satisfies the kinematic boundary condition:

$$R(ar_0, \theta, z) = 0, \quad \Theta(ar_0, \theta, z) = 0, \quad Z(ar_0, \theta, z) = 0, \tag{4}$$

and

$$\forall \delta\mathbf{t} \text{ k.a.}, \quad D\mathcal{E}(\alpha, \mathbf{t})\,[\delta\mathbf{t}] = 0. \tag{5}$$

Here, $D\mathcal{E}(\alpha, \mathbf{t})\,[\delta\mathbf{t}]$ denotes the first variation of the energy evaluated in the configuration $\mathbf{t}$ with an increment $\delta\mathbf{t}$, also known as the first Gâteaux derivative of the functional $\mathcal{E}$ [11].

III. LINEAR ANALYSIS

For the linear stability analysis, we deal with a small perturbation $\varepsilon \mathbf{t}_1$ of the base solution:

$$\mathbf{t} = \mathbf{t}_0 + \varepsilon \mathbf{t}_1 \; = \; (r + \varepsilon u_1(r,\theta,z), \theta + \varepsilon \Theta_1(r,\theta,z), z + \varepsilon z_1(r,\theta,z), q_0 + \varepsilon q_1(r,\theta,z)) \, . \quad (6)$$

Eq.5 writes at order ε^0:

$$D\mathcal{E}(\alpha, \mathbf{t}_0)[\delta \mathbf{t}] = 0, \quad (7)$$

and at order ε:

$$D^2\mathcal{E}(\alpha, \mathbf{t}_0)[\delta \mathbf{t}, \mathbf{t}_1] = 0, \quad (8)$$

where $D^2\mathcal{E}$ is the second Gâteaux derivative of $\mathcal{E}$, which is a bi-linear form on the increment $\mathbf{t}_1$ and on the virtual increment $\delta \mathbf{t}$.

From Eq.7 one obtains (see [4]):

$$q_0 = \frac{\alpha}{2}\left(1 - (r/r_0)^2\right) - 1. \quad (9)$$

In order to deal with order ε, Eq.8, we assume in a standard way a harmonic θ and z dependence of any variation of the perturbation of R, Θ, Z and q:

$$\begin{cases} u_1(r,\theta,z) = \mathcal{R}e\left(f_u(r) e^{\mathrm{i}n\theta + \mathrm{i}kz}\right) \\ \Theta_1(r,\theta,z) = \mathcal{R}e\left(-\mathrm{i} f_\Theta(r) e^{\mathrm{i}n\theta + \mathrm{i}kz}\right) \\ z_1(r,\theta,z) = \mathcal{R}e\left(-\mathrm{i} f_z(r) e^{\mathrm{i}n\theta + \mathrm{i}kz}\right) \\ q_1(r,\theta,z) = \mathcal{R}e\left(f_q(r) e^{\mathrm{i}n\theta + \mathrm{i}kz}\right) \end{cases} \quad (10)$$

where $\mathcal{R}e$ denotes the real part. The conventional complex factor $(-\mathrm{i})$ has been included for convenience, anticipating the fact that the phase of Θ_1 and z_1 is shifted by $\pi/2$ compared to the phase of the other two unknowns. n is the circumferential wave number and k is the axial wave number. Since $R(r,\theta,z) = R(r,\theta+2\pi,z)$, n has to be an integer. Furthermore, from the symmetries $\theta \leftrightarrow -\theta$ and $z \leftrightarrow -z$, one can take n and k positive.

In a previous paper [4] dealing with *homogeneous* spinning (solid) cylinders ($a \to 0$) we have shown that $f_u(r)$ is a solution of the linear differential equation for f_u of order 6:

$$\left(r^6 \frac{\mathrm{d}^2}{\mathrm{d}r^2} + 7r^5 \frac{\mathrm{d}}{\mathrm{d}r} - r^4\left(k^2 r^2 + n^2 - 4n - 5\right)\right) \mathcal{L}^2 f_u = 0, \quad (11)$$

where

$$\mathcal{L} = \frac{\mathrm{d}^2}{\mathrm{d}r^2} + \frac{1}{r}\frac{\mathrm{d}}{\mathrm{d}r} - \left(k^2 + \frac{(n+1)^2}{r^2}\right), \quad (12)$$

with three boundary conditions at $r = r_0$. In the presence of a rigid inner shaft of finite radius ar_0, one has to deal with the three additional kinematic boundary conditions at $r = ar_0$ given by Eqs.4. For a fixed value of the circumferential wave number n, the solutions of Eq.11 can be written as a generalized series expansion

$$f_u(r) = \sum_{m=-\infty}^{\infty} \left(a_m + b_m \ln(kr)\right) (kr)^m, \tag{13}$$

where a_m and b_m depends on the circumferential wave number. For each n, the sequence $(a_m, b_m)_m$ is determined up to six unknown values, that are fixed by the six boundary conditions. Non zero solutions (*i.e.* $(a_m, b_m)_m \neq 0$) exist only for particular values of α that depends on the circumferential wave number n and on the wave number k, $\alpha = \alpha_c(n, k)$ as detailed in Appendix B. For $\alpha = \alpha_c(n, k)$ the straight system is neutrally stable against an infinitesimal perturbation of circumferential wave number n and axial wave number k.

$\alpha_c(0, k)$, $\alpha_c(1, k)$, $\alpha_c(2, k)$, $\alpha_c(3, k)$ are plotted as a function of k in Fig.3 for different values of the dimensionless inner radius a. For $n = 0$ the linear instability threshold $\alpha_c(n = 0, k)$ is minimal for a finite k, and for $n > 0$ and for any a, the linear instability threshold is an increasing function of k. For any a, the absolute minimal value of $\alpha_c(n, k)$ (as a function of n and k) is minimal for a given value of n, $n = n_{\text{first}}$, and $k = 0$ (Fig.4). One concludes that the lower $\alpha_c(n, k)$ is for a prismatic deformation ($k = 0$). Therefore, if one focuses on the first mode that develops upon increasing values of α, one can limit the study to plane-strain deformations. Accordingly, throughout the rest of the article, the wave number is fixed to $k = 0$ and the explicit dependence of any quantity with respect to k is dropped. Taking $k = 0$ (or equivalently $\frac{\partial}{\partial z} = 0$) in the linear analysis, Eq.11 simplifies in [4]:

$$\left(n^2 - 1\right)^2 f_u - \left(2n^2 + 1\right) r \frac{\mathrm{d}f_u}{\mathrm{d}r} + \left(5 - 2n^2\right) r^2 \frac{\mathrm{d}^2 f_u}{\mathrm{d}r^2} + 6r^3 \frac{\mathrm{d}^3 f_u}{\mathrm{d}r^3} + r^4 \frac{\mathrm{d}^4 f_u}{\mathrm{d}r^4} = 0, \tag{14}$$

whose general solution is:

$$f_u = r_0 \left(A \left(\frac{r}{r_0}\right)^{n+1} + B \left(\frac{r}{r_0}\right)^{n-1} + C \left(\frac{r}{r_0}\right)^{1-n} + D \left(\frac{r}{r_0}\right)^{-n-1} \right) \text{ for } n \neq 1, \tag{15}$$

$$f_u = r_0 \left(A \left(\frac{r}{r_0}\right)^{2} + B + C \ln\left(\frac{r}{r_0}\right) + D \left(\frac{r}{r_0}\right)^{-2} \right) \text{ for } n = 1, \tag{16}$$

where A, B, C and D are four constants. With the boundary conditions, one obtains the analytic expression of the linear instability threshold $\alpha = \alpha_c(n)$ as a function on the circumferential mode

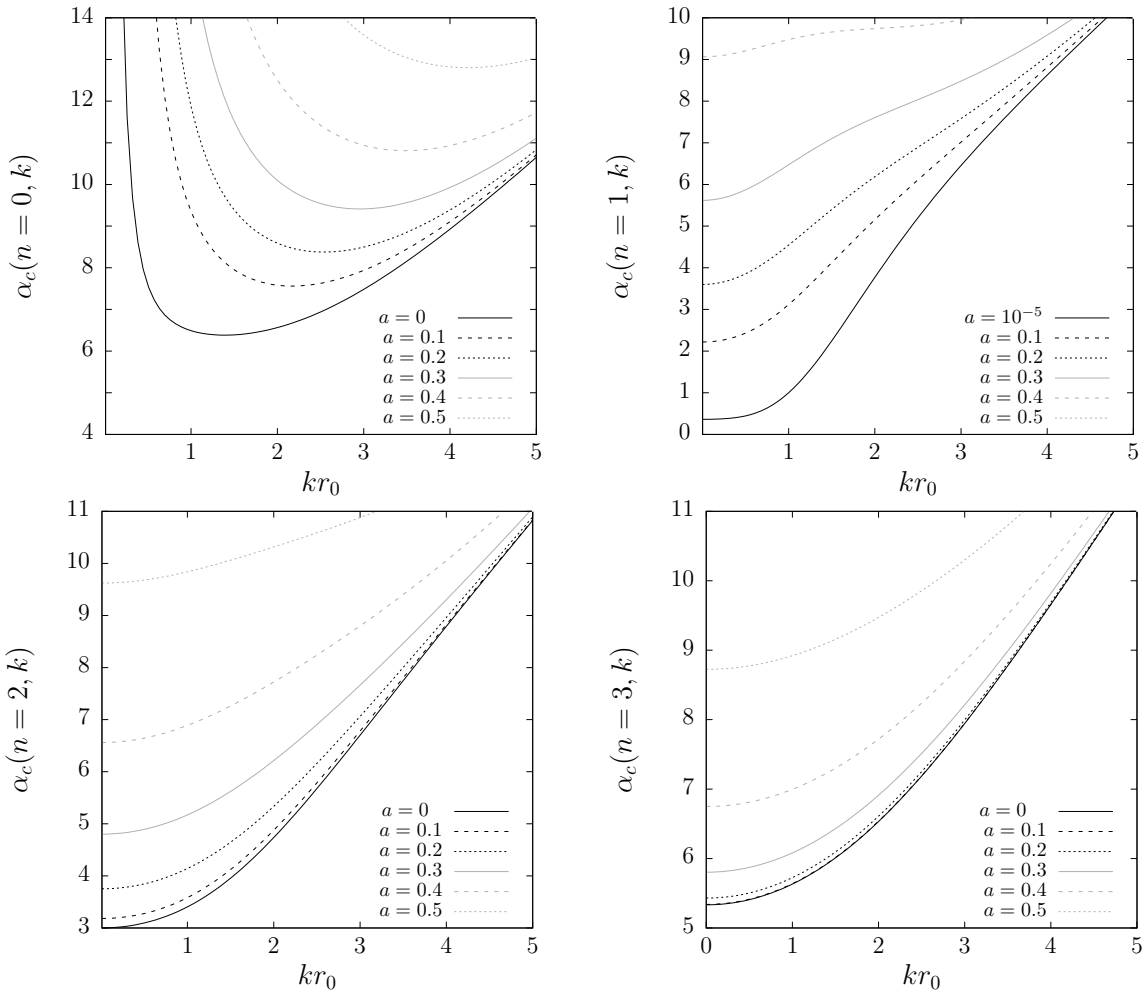

FIG. 3: Critical load parameter for the modes (n,k) at the instability threshold, $\alpha_c(n,k)$, as a function of the dimensionless wave number, kr_0, for the circumferential wave numbers $n=0,1,2,3$ and for various values of the relative radius of the inner cylinder, a.

n and on parameter a (see Appendix A):

$$\alpha_c(n) = \left(\frac{2(n+1)(n-1)}{n}\right)\left(\frac{n^2a^{2n}(a^2-1)^2+a^2(a^{2n}+1)^2}{na^{2n}(a^4-1)+a^2(1-a^{4n})}\right) \quad \text{for} \quad n>1, \tag{17}$$

$$\alpha_c(1) = \frac{8}{\frac{a^4-1}{a^4+1}-2\ln(a)} \quad \text{for} \quad n=1. \tag{18}$$

Fig.4-left shows for various values of parameter a and for different circumferential modes n, the critical load α_c so that mode n is neutrally unstable. Note that $\alpha_c(1)$ for $a=0$ does not lead to a buckled configuration, as it can be anticipated from Eq.16 in which the displacement diverges at $r=0$. This point will be enlightened in Sec. IV.

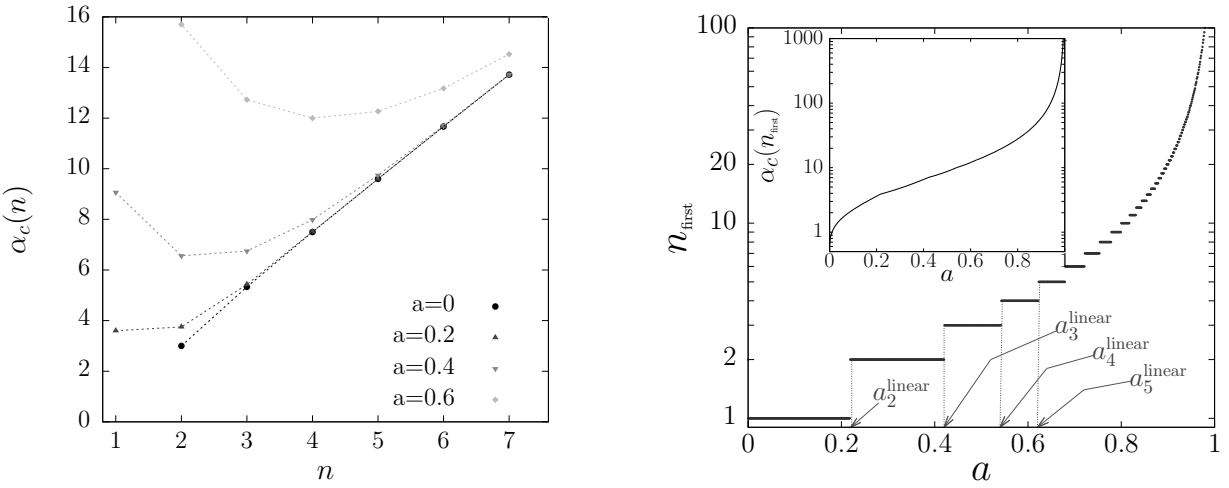

FIG. 4: **Left:** Critical load $\alpha_c(n)$ making the prismatic mode n neutrally unstable, for different values of the dimensionless inner radius a. **Right:** Value of the circumferential wave number n making $\alpha_c(n)$ minimal, for a given value of a. Inset: Threshold value of the load parameter beyond which a mode is unstable, as a function of a.

For a given value of a, we call n_{first} the circumferential wave number n minimizing the critical load $\alpha_c(n)$. It follows that the instability is expected (from the linear analysis) to first appear for $\alpha = \alpha_c(n_{\text{first}})$. The circumferential wave number n_{first} is a discontinuous function of a; it increases step by step as a increases (Fig.4-right). Reciprocally, one defines the sequence $(a_n^{\text{linear}})_n$ so that $n_{\text{first}} = n$ for $a \in [a_n^{\text{linear}}, a_{n+1}^{\text{linear}}]$ (inset of Fig.4). The instability threshold for the prismatic mode with a circumferential wave number $n = 1$ is the lowest if $\alpha_c(1) < \alpha_c(2)$, which defines (from Eqs.18 and 17) the critical value of a, $a_2^{\text{linear}} \simeq 0.218$, below which the first mode to appear is, at linear order, $n = 1$ ($n_{\text{first}} = 1$). a_3^{linear} is defined in the same way by $\alpha_c(2) = \alpha_c(3)$, $a_3^{\text{linear}} \simeq 0.420$: for $a_2^{\text{linear}} < a < a_3^{\text{linear}}$ the first mode to be linearly unstable is the mode with a rotational symmetry of order 2 (invariant under a central rotation of π), $n_{\text{first}} = 2$. The whole sequence $(a_n^{\text{linear}})_n$ is defined as well.

In this section, we have shown that the instability first appears, upon increasing values of the load parameter α, for prismatic modes. The linear instability threshold is for $\alpha = \alpha_c(n_{\text{first}})$, where the function $\alpha_c(n)$ is defined by Eqs.18 and 17. The value of n_{first} depends on the relative radius a of the inner cylinder: the critical radius separating $n_{\text{first}} - 1$ to n_{first}, a_n^{linear}, is determined by the condition $\alpha_c(n_{\text{first}} - 1) = \alpha_c(n_{\text{first}})$.

In the next section, a weakly non linear analysis is carried out in order to capture the amplitude of the buckled modes as a function of the load parameter close to the linear thresholds.

IV. WEAKLY NON LINEAR ANALYSIS

A. Post-bifurcation expansion

Both the load parameter α and the solution $\mathbf{t} = (R, \Theta, q)$ are expanded in terms of the small arc-length parameter ε as:

$$\alpha \;=\; \alpha_{\rm c} + \alpha_2 \varepsilon^2 \tag{19}$$

$$\mathbf{t}(\alpha) \;=\; \mathbf{t}_0(\alpha) + \varepsilon \mathbf{t}_1 + \varepsilon^2 \mathbf{t}_2 + \varepsilon^3 \mathbf{t}_3 + \cdots \tag{20}$$

where $\alpha_c = \alpha_c(n)$ is the critical load from the linear bifurcation analysis (see Eqs.18 and 17), and $\mathbf{t}_1$ is the corresponding linear mode. In the following, the dependence of α_c on n will become implicit in our notation, for the sake of readability. Note that the base solution $\mathbf{t}_0$ depends on the load α through the pressure parameter q_0. The first-order correction $\mathbf{t}_1$ is the linear mode from Section III. The asymptotic post-buckling expansion method [12–18] proceeds by inserting the expansion in Eqs.19–20 into the non linear equilibrium written earlier in Eq.5 as

$$\forall \delta\mathbf{t} \text{ k.a.}, \quad D\mathcal{E}\left(\alpha_{\rm c} + \alpha_2\varepsilon^2, \mathbf{t}_0(\alpha) + \varepsilon\mathbf{t}_1 + \varepsilon^2\mathbf{t}_2 + \varepsilon^3\mathbf{t}_3 + \cdots\right)[\delta\mathbf{t}] = 0, \tag{21}$$

where $\delta\mathbf{t}(r,\theta)$ is the set of virtual functions $\left(\delta R, \delta\Theta, \delta q\right)$ that represent infinitesimal increments satisfying the kinematic boundary conditions. Equation 21 is then expanded order by order in ε [4, 18–20]. At order ε^2, we obtain an equation for $\mathbf{t}_2$,

$$\forall \delta\mathbf{t} \text{ k.a.}, \quad D^2\mathcal{E}(\alpha_{\rm c}, \mathbf{t}_0(\alpha_{\rm c}))\cdot[\mathbf{t}_2, \delta\mathbf{t}] + \tfrac{1}{2}D^3\mathcal{E}(\alpha_{\rm c}, \mathbf{t}_0(\alpha_{\rm c}))\cdot[\mathbf{t}_1, \mathbf{t}_1, \delta t] = 0. \tag{22}$$

At order ε^3, one obtains the equation

$$\begin{aligned}\forall \text{ k.a.}\delta\mathbf{t}, \quad & D^2\mathcal{E}(\alpha_{\rm c}, \mathbf{t}_0(\alpha_{\rm c}))\cdot[\mathbf{t}_3, \delta\mathbf{t}] + D^3\mathcal{E}(\alpha_{\rm c}, \mathbf{t}_0(\alpha_{\rm c}))\cdot[\mathbf{t}_2, \mathbf{t}_1, \delta\mathbf{t}]\cdots \\ & + \alpha_2 \left.\frac{{\rm d}D^2\mathcal{E}(\alpha, \mathbf{t}_0(\alpha))}{{\rm d}\alpha}\right|_{\alpha=\alpha_{\rm c}}\cdot[\mathbf{t}_1, \delta\mathbf{t}] + \frac{1}{6}D^4\mathcal{E}(\alpha_{\rm c}, \mathbf{t}_0(\alpha_{\rm c}))\cdot[\mathbf{t}_1, \mathbf{t}_1, \mathbf{t}_1, \delta\mathbf{t}] = 0.\end{aligned}$$

Upon insertion of the particular virtual displacement $\delta\mathbf{t} = \mathbf{t}_1$, the first term cancels out by Eq.8 and we are left with

$$D^3\mathcal{E}(\alpha_{\rm c}, \mathbf{t}_0(\alpha_{\rm c}))\cdot[\mathbf{t}_2, \mathbf{t}_1, \mathbf{t}_1] + \alpha_2 \left.\frac{{\rm d}D^2\mathcal{E}(\alpha, \mathbf{t}_0(\alpha))}{{\rm d}\alpha}\right|_{\alpha=\alpha_{\rm c}}\cdot[\mathbf{t}_1, \mathbf{t}_1] + \frac{1}{6}D^4\mathcal{E}(\alpha_{\rm c}, \mathbf{t}_0(\alpha_{\rm c}))\cdot[\mathbf{t}_1, \mathbf{t}_1, \mathbf{t}_1, \mathbf{t}_1] = 0. \tag{23}$$

In the equations above, $D^2\mathcal{E}\left[\delta\mathbf{t};\mathbf{t}_1\right]$ denotes the second Gâteaux derivative of $\mathcal{E}$, which is a bi-linear symmetric form on the increment $\mathbf{t}_1$ and on the virtual increment $\delta\mathbf{t}$. Similarly, $D^3\mathcal{E}\left[\delta\mathbf{t};\mathbf{t}_1;\mathbf{t}_2\right]$ is the third Gâteaux derivative (a tri-linear symmetric form).

B. Second order correction to the displacement

The second order displacement $\mathbf{t}_2 = (u_2, \Theta_2, q_2)$ can be computed from Eq.22 with the already known expressions of $\mathbf{t}_0$ and $\mathbf{t}_1$. $\mathbf{t}_1 = (u_1, \Theta_1, q_1)$ is fixed up to a multiplicative constant that defines the buckling amplitude at linear order (Sec. III). In the following, this constant is chosen so that the amplitude of u_1 is ξ:

$$u_1(r_0, \theta) = \xi \cos(n\theta). \tag{24}$$

Eq.23 will be used later (in Sec.IV C) in order to fix the amplitude ξ.

Since $\mathbf{t}_2 = (u_2, \Theta_2, q_2)$ results from the non linear coupling of the linear mode $\mathbf{t}_1$ with itself (Eq.22), it can be expressed as

$$u_2 = \bar{g}_u(r) + \mathcal{R}e\left(g_u(r)e^{2\mathrm{i}n\theta}\right), \tag{25}$$

$$\Theta_2 = \bar{g}_\Theta(r) + \mathcal{R}e\left(-\mathrm{i}g_\Theta(r)e^{2\mathrm{i}n\theta}\right), \tag{26}$$

$$q_2 = \bar{g}_q(r) + \mathcal{R}e\left(g_q(r)e^{2\mathrm{i}n\theta}\right), \tag{27}$$

where g_u, g_Θ and g_q are second order complex amplitudes that are functions of r only, and $\bar{g}_u$, $\bar{g}_\Theta$ and $\bar{g}_q$ represent the constant terms in u_2, Θ_2 and q_2 respectively, which are also functions of r.

Inserting the expressions $\mathbf{t}_0$ and $\mathbf{t}_1$ in Eq.22, one obtains in strong form a set of seven equations: the incompressibility constraint, the equilibrium in the radial and circumferential directions, the kinematic condition at $r = ar_0$ and the boundary equations at $r = r_0$, in the radial and circumferential directions. Each equation can be separated in two parts : one is independent of θ and involves $\bar{g}_u$, $\bar{g}_\Theta$ and $\bar{g}_q$. The other part depends on θ and involves g_u, g_Θ and g_q. The derivation as well as the resolution of these equations are detailed in Appendix C for an isotropic and incompressible neo-Hookean material for which, in the plane-strain problem we consider here, $W = 1/2\,(I_1 - 3)$.

In the following, we focus on materials that follow this constitutive law. Note that for an incompressible material, the neo-Hookean model is equivalent to the Mooney-Rivlin constitutive law in plane-strain deformation [21]. This study is therefore also relevant for any incompressible Mooney-Rivlin solid.

C. Determination of the amplitude of mode n

$D^2\mathcal{E}(\alpha, \mathbf{t}_0(\alpha)) \cdot [\mathbf{t}_1, \mathbf{t}_1]$, $D^3\mathcal{E}(\alpha_c, \mathbf{t}_0(\alpha_c)) \cdot [\mathbf{t}_2, \mathbf{t}_1, \mathbf{t}_1]$ and $D^4\mathcal{E}(\alpha_c, \mathbf{t}_0(\alpha_c)) \cdot [\mathbf{t}_1, \mathbf{t}_1, \mathbf{t}_1, \mathbf{t}_1]$ are calculated with the help of a symbolic calculation language and without any approximation, as a function of r_0, a, n and ξ from the expressions of f_u, f_Θ, f_q, g_u, g_q, g_Θ, $\bar{g}_u$, $\bar{g}_q$ and $\bar{g}_\Theta$ introduced in Sections III and IV. Since $\mathbf{t}_1$ is proportional to ξ and $\mathbf{t}_2$ is proportional of ξ^2, the second Gâteaux derivative aforementioned is proportional to ξ^2, the third and the fourth Gâteaux derivative in Eq.23 are proportional to ξ^4. One obtains from Eq.23 a relation between ξ, a, n and α_2 in the form:

$$\left(\frac{\xi}{r_0}\right)^2 \left(\alpha_2 - f_n(a) \left(\frac{\xi}{r_0}\right)^2\right) = 0, \tag{28}$$

with $f_n(a)$ a function of a whose exact expression is too cumbersome to be written here. $f_1(a)$ and $f_2(a)$ are plotted in Fig.5. $f_n(a)$ is plotted in Fig.6 for $n = 1, ..., 6$ together. f_1 is negative for

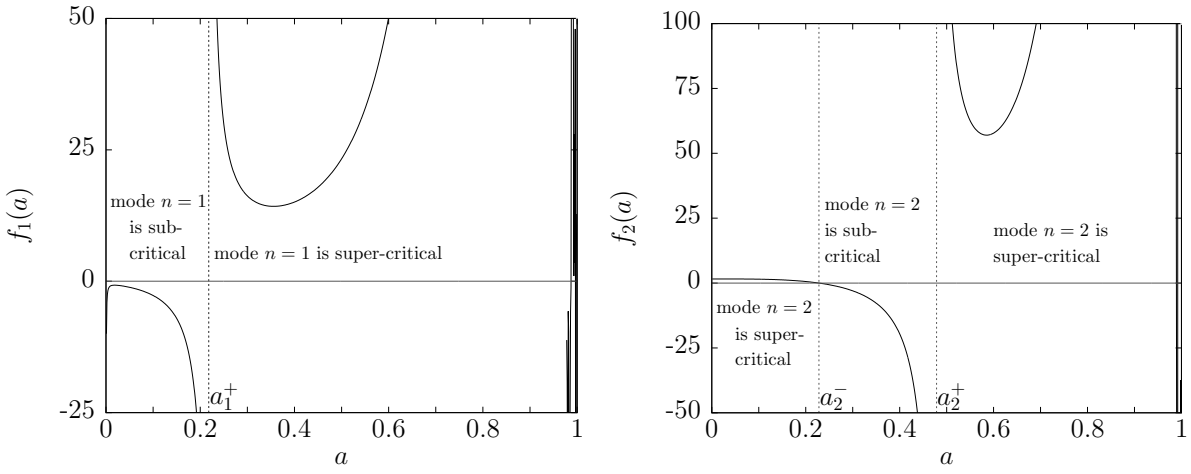

FIG. 5: f_1 (left) and f_2 (right) as a function of a, calculated from the analytic expressions deduced from Eq.23.

a in the range $[0, a_1^+]$ with $a_1^+ \simeq 0.218$. Then f_1 is positive and change again of sign for a close to 1 (see Fig.5(left)). The variations of functions $f_n(a)$ have the same structure than $f_2(a)$ for any $n > 1$ (see Fig.6): $f_n(a)$ is positive in the range $[0, a_n^-]$ with $a_n^- \in]0, 1[$. It is negative in $[a_n^-, a_n^+]$. It is then positive until a value of a close to 1. In Fig.6 the vertical axis is zoomed in order to focus on the first zero of the functions f_n.

We define the true buckling amplitude ζ as the amplitude of the displacement $\mathbf{R} - \mathbf{r}$. At linear order, $\zeta = \varepsilon\, \xi$. With Eqs.19, 24 and 20, one obtains from Eq.28 the relation (at order ε) between ζ

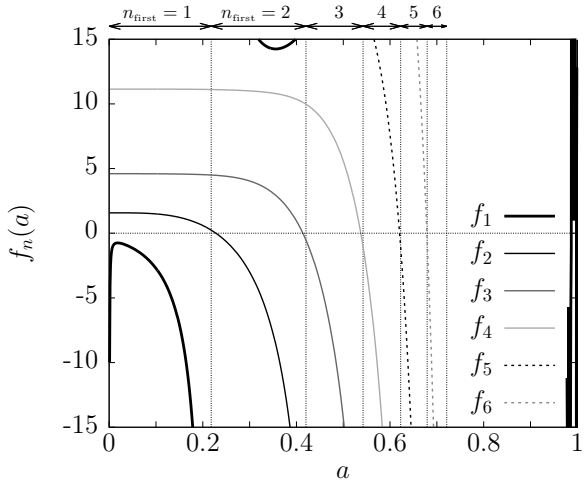

FIG. 6: f_n as a function of a for $n = 1, 2, 3, 4, 5, 6$, calculated from the analytic expressions deduced from Eq.23.

and $\alpha - \alpha_c$:

$$\frac{\zeta^2}{r_0^2} = \frac{\alpha - \alpha_c}{f_n(a)} \text{ or } \zeta = 0. \tag{29}$$

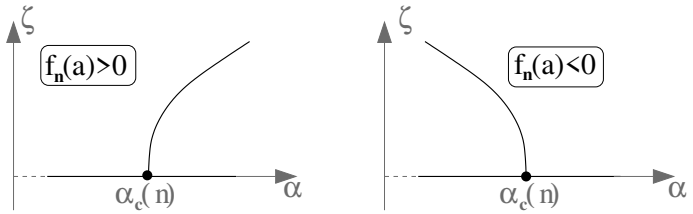

FIG. 7: Scheme of the true buckling amplitude ζ for a fixed circumferential wave number n as a result of Eq.23. In any case $\zeta = 0$ is a solution. **Left:** If $f_n(a) > 0$ then a non zero solution exists for $\alpha > \alpha_c(n)$ with $\zeta = r_0/\sqrt{f_n(a)} \times \sqrt{\alpha - \alpha_c(n)}$. **Right:** If $f_n(a) < 0$ then a non zero solution exists for $\alpha < \alpha_c(n)$ with $\zeta = r_0/\sqrt{-f_n(a)} \times \sqrt{\alpha_c(n) - \alpha}$.

From Eq.29, $\alpha - \alpha_c$ and $f_n(a)$ have the same sign: $\alpha > \alpha_c$ for $f_n(a) > 0$ and $\alpha < \alpha_c$ for $f_n(a) < 0$. One concludes that depending on the sign of $f_n(a)$, hence on the circumferential wave number and on the relative inner radius, the bifurcation can be super-critical ($f_n(a) > 0$) or sub-critical ($f_n(a) < 0$), see Fig.7. As a consequence, the mode $n = 1$ is sub-critical for $a < a_1^+$, and is super-critical for a in a wide range beyond a_1^+. A mode $n \geq 2$ is super-critical for $a < a_n^-$ and

sub-critical for $a_n^- < a < a_n^+$.

A summary list of the critical inner radii introduced above, with their definition, is provided in Appendix D.

D. Discussion

We focus on the transition from the unbuckled to the first buckled configuration, *i.e.* on the first mode that appears upon increasing values of α. Interesting features of the bifurcation (as the instability threshold and the critical nature of the transition) can be deduced from the comparison of the sequences $(a_n^-)_n$, $(a_n^+)_n$ and $(a_n^{\text{linear}})_n$. Note that for a reason that is unclear for us, $a_1^+ = a_2^{\text{linear}}$.

- For dimensionless radius $a < a_1^+ \simeq 0.218$, $f_1(a) < 0$ and $f_n(a) > 0$ for any circumferential wave number $n > 2$ (Fig.8). Modes with $n \geq 2$ will therefore not develop first since they appear for a load $\alpha > \alpha_c(n) > \alpha_c(1)$. From the negative sign of $f_1(a)$ we deduce that the bifurcation is sub-critical with the true buckling amplitude $\zeta = \frac{r_0}{\sqrt{-f_1(a)}}\sqrt{\alpha_c(1) - \alpha}$ (Fig.9-a). Note that for $a = 0$, the unique solution of Eq.28 is $\xi = 0$ since α_2 is in this case always positive ($\alpha_c(1) = 0$).

- Let us consider systems with a thinner compliant layers, the relative radius a being such that $a_1^+ < a < a_2^- \simeq 0.228$. In this case $f_n(a) > 0$ for any n (Fig.8) and the bifurcation is super-critical. Since in this range of a, $n_{\text{first}} = 2$, the mode with a rotational symmetry of order 2 develops first with the true buckling amplitude $\zeta = \frac{r_0}{\sqrt{f_2(a)}}\sqrt{\alpha - \alpha_c(2)}$ (Fig.9-b).

- For systems with a such that $a_2^- < a < a_3^- \simeq 0.414$, $n_{\text{first}} = 2$, $f_2(a) < 0$ and $f_{n\neq 2}(a) > 0$ (Fig.8). One concludes that the bifurcation is sub-critical and appears with mode $n = 2$.

- For systems with a such that $a_3^- < a < a_2^+ \simeq 0.478$, $f_2(a) < 0$, $f_3(a) < 0$ and the others $f_n(a)$ are positive (Fig.8). Moreover $n_{\text{first}} = 2$ or $n_{\text{first}} = 3$. The bifurcation is then sub-critical and appears either with mode $n = 2$ or mode $n = 3$. One cannot discriminate between $n = 2$ or $n = 3$ from the weakly non linear analysis (Fig.9-c and Fig.11).

- For systems with a such that $a_2^+ < a < a_4^- \simeq 0.538$, $n_{\text{first}} = 3$, $f_3(a) < 0$, $f_{n\neq 3(a)} > 0$ (Fig.8). The bifurcation is therefore sub-critical and the mode $n = 3$ develops (Fig.9-d).

- For systems with a such that $a_4^- < a < a_3^+ \simeq 0.612$, $f_3(a) < 0$, $f_4(a) < 0$ and the other $f_n(a)$ are positive (Fig.8). In this case $n_{\text{first}} = 3$ or $n_{\text{first}} = 4$: the bifurcation is sub-critical

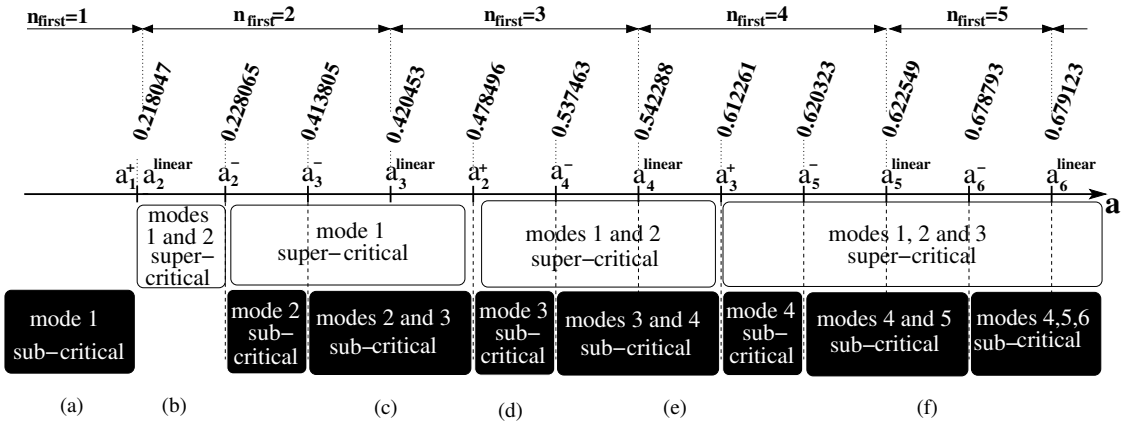

FIG. 8: Partial summary of the instability structure emerging from the weakly non linear analysis, as a function of the dimensionless inner radius a. The amplitudes of the two modes with the smallest $\alpha_c(n)$ for the values of a indicated by (a), (b), (c), (d), (e) and (f) are plotted in Fig.9. Note that the scale of the axis of a is not linear.

with $n = 3$ or $n = 4$ (Fig.9-e). One cannot discriminate between $n = 3$ or $n = 4$ from the weakly non linear analysis.

- For $a_3^+ < a < a_5^- \simeq 0.620$, $f_4(a) < 0$ and $f_{n\neq 4}(a) > 0$. In addition $n_{\text{first}} = 4$ (Fig.8): the bifurcation is sub-critical with $n = 4$.

- The structure of instability can be determined in the same way for the larger values of the dimensionless inner radius a.

To conclude, the weakly non linear post-buckling expansion unambiguously predicts whether the transition of the straight rotating cylinder toward the buckled configuration is sub-critical or super-critical. In the case one mode is sub-critical, *e.g.* mode n_1, the post-buckling expansion we have considered is not suitable in order to determine the smallest value of α at which this mode starts to develop. Indeed, the buckled configuration exists in this case for some values of α smaller than $\alpha_c(n_1)$, but the weakly non linear post buckling expansion tells us nothing about the corresponding range of α. This is the reason why an uncertainty may subsist in certain cases about the value of the instability threshold and/or the order in the rotational symmetry of the resulting pattern. One needs to deal with finite deformations in order to address these issues, which is done below with simulations using the finite element method (Sec. V).

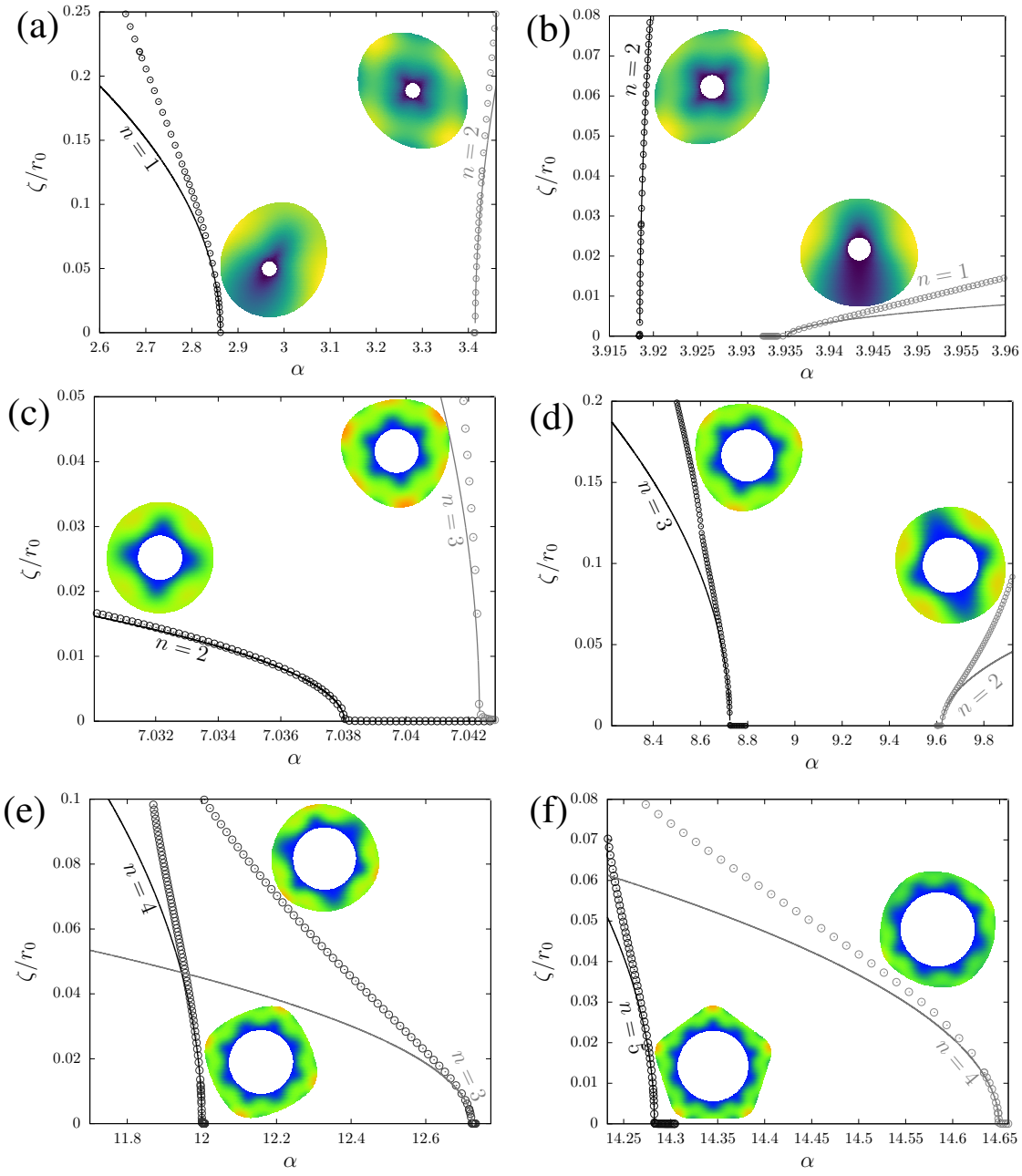

FIG. 9: Amplitudes ζ of modes of deformation as a function of the load parameter α, for different relative radius of the inner cylinder (values of a are 0.15, 0.22, 0.42, 0.5, 0.6, 0.65 in figs (a), (b), (c), (d), (e) and (f) respectively). Solid lines are for amplitudes computed from the analytic expression Eq.29. Empty circles and the snapshots originate from finite element simulations of Section V. The amplitude of the unstable mode with the lowest value of α_c is in black (circumferential wave numbers are respectively $n_{\text{first}} = 1, 2, 2, 3, 4$ and 5), and the amplitude of the second mode with the lowest value of α_c is in gray (circumferential wave numbers are respectively $n = 2, 1, 3, 2, 3$ and 4). The other modes are not shown in these figures. Deformed shapes obtained by simulations are shown in the insets ; the color map represents the magnitude of the displacement increasing from blue (no displacement) to orange.

V. BEYOND THE WEAKLY NON LINEAR ANALYSIS

In this section we numerically implement the complete non linear problem defined by Eq.5 by using the open source tool for solving partial differential equations FEniCS [22]. In a first step, we show that the numerical simulations that we have implemented capture well the results of the linear analysis and the non linear analysis (Sec. V A). Then we present the results obtained beyond the validity range of the weakly non linear analysis (Sec. V B).

A. Finite element implementation

We consider a 2-dimensional corona Ω_a of inner and outer radii equal respectively to ar_0 and r_0 ($0 < a < 1$). A Cartesian coordinates system (x, y) with the base vectors $(\mathbf{e}_x, \mathbf{e}_y)$ is chosen such that $(x, y) \in \Omega_a \Leftrightarrow a < r/r_0 < 1$, with $r = \sqrt{x^2 + y^2}$. An incompressible and isotropic neo-Hookean elastic solid occupying the domain Ω_a in its reference configuration is subjected to the action of the centrifugal volume force $\alpha(x\mathbf{e}_x + y\mathbf{e}_x)/r$. The inner surface is prescribed to have zero displacement and the outer one is traction free. The non linear problem in $\mathbf{u} - q$, with $\mathbf{u}$ the displacement vector and q the Lagrange multiplier, is solved using a Newton algorithm based on a direct parallel solver (`MUMPS`). Quasi-static simulations are performed by setting $\mu = 1$, $r_0 = 1$, and slowly varying α up to the desired value. For each α the displacement field, the Lagrange multiplier and the total energy of the system (taking for the energy reference the base state) are computed.

Starting from the undisturbed system ($\mathbf{u} = 0$), α is gradually increased or decreased (with increments $\delta\alpha = 1/4000$). A spatially uncorrelated random disturbance of maximal amplitude $\xi_0 = 10^{-3}$ is added before each step in order to trigger the instability. Due to its small amplitude, the random disturbance no longer plays a role once the instability has begun to develop. Simulations have been carried out for different values of the relative inner radius a and different values of the linear mesh density n_{mesh}. Depending on the initial value of α, on a and on n_{mesh} the instability develops below (as in Figs. 9-a,c,d,e,f) or beyond (as in Figs. 9-a,b,d) a critical load $\alpha^*(n_{mesh})$. The convergence of $\alpha^*(n_{mesh})$ with the linear mesh density n_{mesh} is shown in Fig.10 for $a = 0.44$. The limit $\alpha^*(n_{mesh} \to \infty)$ is consistent with the analytical prediction (Eqs.18 and 17), with a residual error well below 10^{-4}.

The true buckling amplitude ζ defined in Sec. IV C, *i.e.* the amplitude of the displacement

$\mathbf{R}-\mathbf{r}$, is computed from the simulations as $\zeta = \frac{1}{2}(R_{max}/R_{min} - 1)$, where R_{min} and R_{max} are the smallest and largest distance from the deformed lateral boundary to the origin. This amplitude ζ is plotted as a function of α in Figs. 9 for different values of a, and compared to the prediction based on the weakly non linear post buckling expansion (Eqs.29). The agreement is good in the limit of the small amplitudes, which indeed corresponds to the domain of validity of the post-buckling expansion.

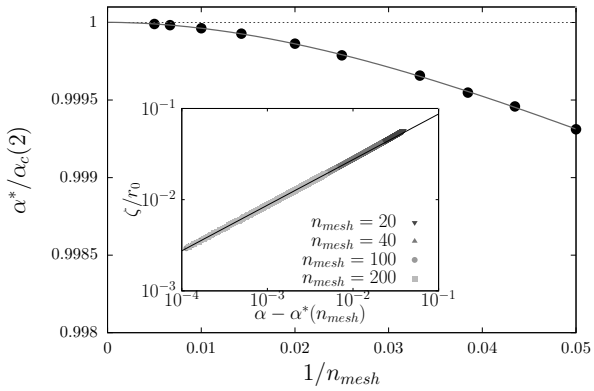

FIG. 10: Critical load parameter α^* arising from non linear finite element simulations of a system with the relative inner radius $a = 0.44$. The simulations have been carried out with different values of the linear mesh density, n_{mesh}. **Inset:** Dimensionless amplitude ζ/r_0 plotted in log-log scales as a function of $\alpha^* - \alpha^*(n_{mesh})$ for different values of n_{mesh}. The solid line, calculated from Eq.29 is the prediction arising form the post-buckling expansion. The collapse of the curves indicated a weak dependence of the exponent and the prefactor in $\zeta/r_0 = (\alpha^*(n_{mesh}) - \alpha)^p$ with the mesh density.

B. Post-buckling analysis

The simulations provide a solution beyond the range of validity of the weakly non linear post-buckling expansion used in Sec. IV. From the post-buckling expansion developed in Sec. IV, we have unambiguously demonstrate whether the instability of the straight cylinder is super-critical or sub-critical : we have shown that the bifurcation is super-critical for $a_1^+ < a < a_2^-$, and sub-critical elsewhere.

For $a_1^+ < a < a_2^-$ the threshold is $\alpha_c(2)$ as calculated with Eq.17, and the circumferential wave number is $n = 2$, *i.e.* the order of the rotational symmetry in the buckled configuration is 2. In contrast, for $a < a_1^+$ the transition is sub-critical and the weakly non linear post-buckling

expansion is not enough to find the lower value of α at which an unstable mode first exists. Note that in this case the only mode that will first occur consists in a continuation of mode $n = 1$ since the other modes ($n = 2, 3, 4, ...$) are super-critical with a larger linear threshold. For $a_3^- < a < a_2^+$, both modes $n = 2$ and $n = 3$ are sub-critical, and then one does not know which one of these two modes appears first. For $a_2^+ < a < a_4^-$, mode $n = 3$ is sub-critical ; the other modes are super-critical and then, the order of the rotational symmetry in the buckled configuration is 3.

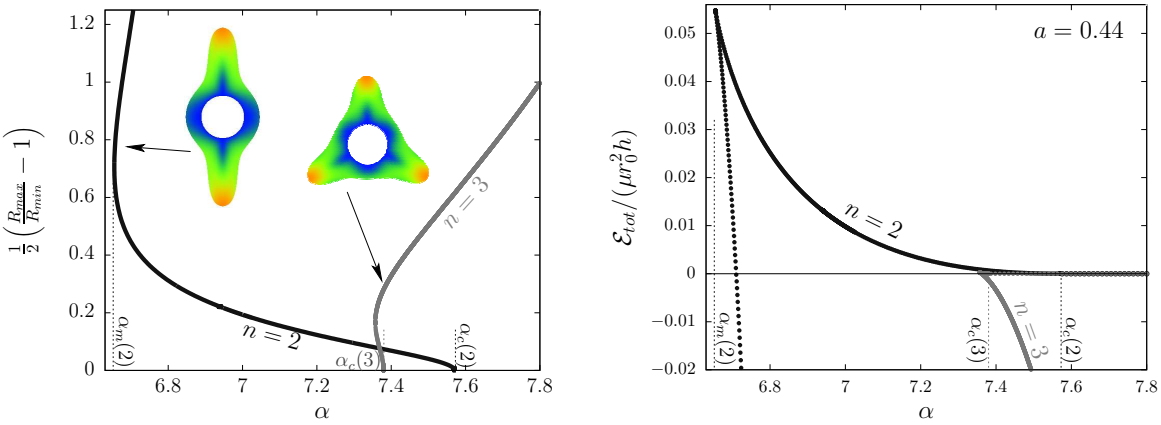

FIG. 11: **Left -** True buckling amplitude ζ as a function of the load parameter α for $a = 0.44$ computed for deformations with rotational symmetry of order $n = 2$ and $n = 3$, which corresponds to the two lowest values of α at the linear threshold. Since for this value of a the modes with circumferential wave numbers $n = 2$ and $n = 3$ are sub-critical, the buckled configurations start to develop bellow the linear thresholds, respectively $\alpha_c(2)$ and $\alpha_c(3)$. Deformed shapes obtained by simulations are shown in the insets ; the color map represents the magnitude of the displacement increasing from blue (no displacement) to orange. **Right -** Dimensionless energy of the system as a function of α.

In the following, we use finite element simulations beyond the domain of validity of the weakly non linear post-buckling expansion in order to determine the lowest value of α for which the instability occurs (for a given value of a) through the hypothesis of plane-strain deformations. Let us consider a value of a so that the bifurcation is sub-critical. Upon decreasing α from the linear threshold toward lower values, the computed true amplitude ζ of a mode with rotational symmetry of order n increases as well as the associated energy (Fig.11), until a particular value of α at which the slope of ζ versus α is infinite. We call $\alpha_m(n)$ the corresponding value of α. No buckled solution is found for $\alpha < \alpha_m(n)$. Increasing now α from $\alpha_m(n)$ toward larger values, the true buckling amplitude ζ again increases. The total energy is found to increase as α decreases during

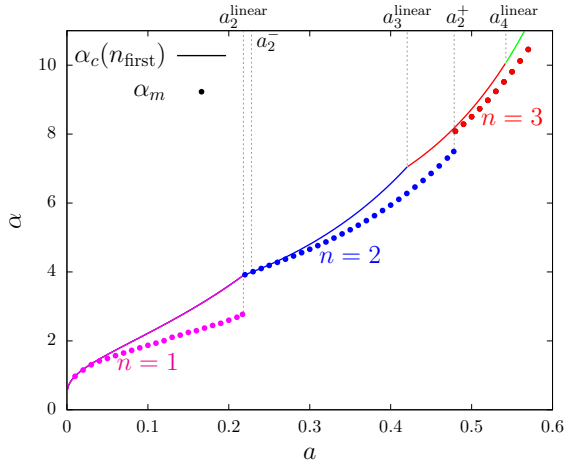

FIG. 12: Instability threshold as a function of a, considering deformations with rotational symmetry of order 1 ($n = 1$, magenta), order 2 ($n = 2$, blue) and order 3 ($n = 3$, red) for a in the range $[0.05, 0.58]$. Filled circles are for the minimal value of α, α_m, for which a buckled solution exists. Continuous lines are for $\alpha_c(n_{\text{first}})$ calculated from Eqs.18 and 17.

the first step (from $\alpha^*(n_{mesh})$ to α_m), and to decrease as α increases beyond α_m in the second step, reaching negative values beyond a certain $\alpha > \alpha_m(n)$ (Fig.11-right). The solutions corresponding to the first step (from $\alpha^*(n_{mesh})$ to α_m) are unstable, while the solutions corresponding to the second step (α increases beyond α_m) are stable [4, 23, 24].

As a consequence, even if the energy is positive, *i.e.* higher than the energy of the base state, a stable buckled solution exists for $\alpha > \alpha_m$. $\alpha_m(n)$ is the lowest possible value of the load parameter α for a non zero solution with a rotational symmetry of order n. If now the rotational symmetry n corresponds to a supercritical mode, the lowest value of α so that de deformation with this symmetry develops is obviously $\alpha_m(n) = \alpha_c(n)$.

For a fixed value of the dimensionless inner radius a, the first deformation that can develop is therefore the deformation with the rotational symmetry of order n having the lowest $\alpha_m(n)$. For example in Fig.11 where $a = 0.44$, one observes that, even if $\alpha_c(2) > \alpha_c(3)$ (*i.e.* $n_{\text{first}} = 3$), $\alpha_m(3) > \alpha_m(2)$: the order in the rotational symmetry of the deformation that appears upon increasing α is therefore 2. For given values of a, a systematic comparison of $\alpha_m(n)$ for different n yields the absolute instability threshold, α_m, of the system. α_m is plotted as a function of a together with $\alpha_c(n_{\text{first}})$ in Fig.12, for a in the range $[0.05, 0.58]$. α_m is smaller than $\alpha_c(n_{\text{first}})$ except for $a \in [a_2^{\text{linear}}, a_2^-]$ since the instability is super-critical in this case. The order in the rotational

symmetry is equal to $n = 1$ for $0 < a < a_2^{\text{linear}}$, it is equal to $n = 2$ for $a_2^- < a < a_2^+$: the uncertainty over the order in the rotational symmetry for $a_3^- < a < a_2^+$ is then now fixed. Strikingly, the absolute threshold α_m is not a continuous function of a, since one observes a jump for $a = a_2^{\text{linear}}$ and $a = a_2^+$.

The different critical control parameters α defined above are summarized, together with the critical inner radii, in Appendix D.

VI. CONCLUDING REMARKS

The bifurcations in cylinders consisting in a rigid shaft surrounded by an homogeneous and incompressible elastic hollow cylinder rotating about their axis, have been investigated. They arise at critical load parameters that depend on the geometry (through the relative radius of the rigid shaft, a), on the mass density of the hollow cylinder, its shear modulus, and the angular velocity square.

The complete linear analysis shows that this 3-dimensional system can be reduced, for the weakly non linear regime, to a plane-strain formulation. While the stability analysis we propose is valid for any elastic constitutive law, our weakly non linear analysis has been carried out for a Mooney-Rivlin constitutive law for the sake of simplicity, which exactly coincides to the neo-Hookean form in this plane-strain problem. As a consequence, the unique relevant elastic parameter is the shear modulus μ, and no additional material constant is needed. Within this hypothesis, the bifurcation is super-critical for systems with $0.218 < a < 0.228$, and sub-critical elsewhere. The corresponding buckling amplitude has been calculated at order $|\alpha - \alpha_c|^{1/2}$, with α_c the critical load parameter calculated from the linear analysis and α the actual load parameter. The agreement with finite element simulations is excellent. In case of sub-critical bifurcations leading to configurations with rotational symmetry of order n, a weakly non linear analysis cannot predict the lowest possible value of the load parameter ($\alpha_m(n)$) at which these buckled configurations can develop, because the corresponding deformations are finite. $\alpha_m(n)$ has then been computed by means of finite element simulations. For a given value a of the relative inner radius, minimizing $\alpha_m(n)$ with respect to n gives the lowest load parameter for a buckled configuration, with the corresponding order n of the rotational symmetry.

Indeed, the buckling amplitude as well as the range in which the bifurcation is super/sub-

critical depend on the precise constitutive law that may deviate from the Mooney-Rivlin model for certain rubber-like materials. Following [4], one postulates that the post-buckling behavior of such system with an arbitrary elastic constitutive law for the elastic hollow cylinder can be captured, at least qualitatively, by replacing the modulus μ in the prediction of the neo-Hookean model by the apparent modulus $\mu_{\rm app}$ defined (for plane-strain deformations) as:

$$\mu_{\rm app}(I_1) = 2\mu \frac{W(I_1)}{I_1 - 3}, \tag{30}$$

where $\mu_{\rm app}$ is evaluated for $I_1 = \langle I_1 \rangle$, the mean value of the first invariant I_1 calculated within the neo-Hookean model. Following this way, our results can be extended to any constitutive law of an incompressible elastic material.

In the limit of thin hollow cylinders this instability is closely related to the elastic Rayleigh-Taylor instability [18, 25–27]. Our control parameter α can be rewritten as

$$\alpha = \frac{1}{1-a} \cdot \frac{\rho\,(r_0\omega^2)\,h}{\mu}, \tag{31}$$

where $h = (1-a)r_0$ is the thickness of the cylindrical shell and $r_0\omega^2$ is the acceleration at the outer surface. The critical value of the dimensionless acceleration at the outer surface, $\rho\,(r_0\omega^2)\,h/\mu$ computed from Eq. 17, tends to the threshold value $\simeq 6.223$, which exactly corresponds to the linear threshold of the Rayleigh-Taylor instability of an initially flat elastic layer. The thin layer limit has not been investigated in the weakly non linear regime in details in this article. The reader interested by this limit can refer to [4].

The changes of the mechanical properties resulting from these bifurcations are expected to occur in systems with joints, insulators or adhesives placed in between rotating pieces of machine rotating at high angular velocity. They can be important for the stability of these complex systems. This instability can also be used as a route to produce regular cylindrical patterns with a well defined and controlled geometry.

---

[1] J.C. Patterson and J.M. Hill. The stability of a solid rotating neo-hookean cylinder. *Mech. Res. Comm.*, 4:69–74, 1977.

[2] D.M. Haughton and R.W. Ogden. Bifurcation of finitely deformed rotating elastic cylinders. *Q. J. Mech. appl. Math.*, 33:251–265, 1980.

[3] P.J. Rabier and J.T. Oden. *Bifurcation in rotating bodies*. Masson Springer-Verlag, Paris, 1989.

[4] F. Richard, A. Chakrabarti, B. Audoly, Y. Pomeau, and S. Mora. Buckling of a spinning elastic cylinder: linear, weakly nonlinear and post-buckling analyses. *Proc. Roy. soc. A*, 474:20180242, 2018.

[5] J. Padovan and O. Paramodilok. Generalized solution of time dependent traveling load problem via moving finite element scheme. *Journal of Sound and Vibration*, 91:195–209, 1983.

[6] J.T. Oden and T.L. Lin. On the general rolling contact problem for finite deformations of a viscoelastic cylinder. *Computer Methods in Applied Mechanics and Engineering*, 57:297–367, 1986.

[7] A. Chatterjee, J.P. Cusumano, and J.D. Zolock. On contact-induced standing waves in rotating tires: Experiment and theory. *Journal of Sound and Vibration*, 227:1049–1081, 1999.

[8] V.V. Krylov and O. Gilbert. On the theory of standing waves in tyres at high vehicle speeds. *Journal of Sound and Vibration*, 329:4398–4408, 2010.

[9] S. Govindjee, T. Potter, and J. Wilkening. Dynamic stability of spinning viscoelastic cylinders at finite deformation. *International Journal of Solids and Structures*, 51:3589–3603, 2014.

[10] Le Tallec P. and C. Rahler. Numerical models of steady rolling for nonlinear viscoelastic structures in finite deformations. *Int. J. for Numerical Methods in Eng.*, 37:1159–1186, 1994.

[11] R. Gâteaux. Fonctions d'une infinité de variables indépendantes. *Bulletin de la Société Mathématique de France*, 47:70–96, 1919.

[12] W. T. Koiter. *On the Stability of an Elastic Equilibrium*. PhD thesis, Delft; H. J. Paris, Amsterdam, The Netherlands, 1945.

[13] J. W. Hutchinson. Imperfection sensitivity of externally pressurized spherical shells. *Journal of Applied Mechanics*, 34:49–55, 1967.

[14] J. W. Hutchinson and W.T. Koiter. Postbuckling theory. *Applied Mechanics Reviews*, pages 1353–1366, 1970.

[15] B. Budiansky. Theory of buckling and post-buckling behavior of elastic structures. *Advances in applied mechanics*, 14:1–65, 1974.

[16] R. Peek and N. Triantafyllidis. Worst shapes of imperfections for space trusses with many simultaneously buckling members. *International Journal of Solids and Structures*, 29:2385–2402, 1992.

[17] R. Peek and M. Kheyrkhahan. Postbuckling behavior and imperfection sensitivity of elastic structures

by the Lyapunov-Schmidt-Koiter approach. *Computer methods in applied mechanics and engineering*, 108(3):261–279, 1993.

[18] A. Chakrabarti, S. Mora, F. Richard, T. Phou, J.-M. Fromental, Y. Pomeau, and B. Audoly. Selection of hexagonal buckling patterns by the elastic Rayleigh-Taylor instability. *Journal of the Mechanics and Physics of Solids*, 121:234–257, 2018.

[19] A. van der Heijden. *W. T. Koiter's elastic stability of solids and structures*. Cambridge University Press Cambridge, 2009.

[20] Nicolas Triantafyllidis. *Stability of solids: from structures to materials*. Ecole Polytechnique, 2011.

[21] M. Destrade, M.D. Gilchrist, and J.G. Murphy. Onset of non-linearity in the elastic bending of blocks. *ASME Journal of Applied Mechanics*, 77:061015, 2010.

[22] A. Logg, K.A. Mardal, and G. Wells. *Automated Solution of Differential Equations by the Finite Element Method*. Springer, 2012.

[23] C. Normand, Y. Pomeau, and M. G. Velarde. Convective instability: a physicist's approach. *Reviews of Modern Physics*, 49(3):581, 1977.

[24] S. Strogatz. *Non-linear Dynamics and Chaos: With applications to Physics, Biology, Chemistry and Engineering*. Addison-Wesley, 1994.

[25] S. Mora, T. Phou, J. M. Fromental, and Y. Pomeau. Gravity driven instability in solid elastic layers. *Phys. Rev. Lett.*, 113:178301, 2014.

[26] X. Liang and S. Cai. Gravity induced crease-to-wrinkle transition in soft materials. *Appl. Phys. Lett.*, 106:041907, 2015.

[27] D. Riccobelli and P. Ciarletta. Rayleigh-taylor instability in soft elastic layers. *Phil. Trans. R. soc. A*, 375:20160421, 2017.

[28] See supplementary material.

Appendix A: Linear analysis for prismatic deformations

In this appendix, the main steps leading to the expression of the linear instability threshold (Eqs.17 and 18) are introduced. Then, the complete expression of the first order displacement is given.

The fourth order linear equation Eq.14, with the zero traction condition at the lateral boundary,

Eqs.(3.7) of [4], have to be completed with the zero displacement condition at the inner interface of the elastic layer, $f_u(ar_0) = 0$ and $f_\Theta(ar_0) = 0$.
These boundary conditions write:

$$\left(\frac{1}{r_0} - \frac{n^2}{r_0} - \frac{n^2\alpha}{r_0}\right) u + \left(3n^2 - 1\right) \frac{\mathrm{d}u}{\mathrm{d}r} - 4r_0 \frac{\mathrm{d}^2u}{\mathrm{d}r^2} - r_0^2 \frac{\mathrm{d}^3u}{\mathrm{d}r^3} = 0 \quad \text{at} \quad r = r_0, \tag{A1}$$

$$\left(n^2 - 1\right) u + r_0 \frac{\mathrm{d}u}{\mathrm{d}r} + r_0^2 \frac{\mathrm{d}^2u}{\mathrm{d}r^2} = 0 \quad \text{at} \quad r = r_0, \tag{A2}$$

$$u = 0 \quad \text{at} \quad r = ar_0, \tag{A3}$$

$$\frac{\mathrm{d}u}{\mathrm{d}r} = 0 \quad \text{at} \quad r = ar_0. \tag{A4}$$

The general solution of Eq.14 is given by Eq.16 if $n = 1$ and by Eq.15 for $n > 1$. Inserting these expressions in Eqs.A1-A4, one obtains a linear system of 4 homogeneous equation with four unknowns. A non zero solution of this system exists if the determinant of this system is zero. For $n > 1$ this condition is:

$$\begin{vmatrix} \left(n^2 - n - 2 - \frac{n\alpha}{2}\right) & \left(n(n-1) - \frac{n\alpha}{2}\right) & \left(-n^2 - n + 2 - \frac{n\alpha}{2}\right) & \left(-n(n+1) - \frac{n\alpha}{2}\right) \\ n+1 & n-1 & n-1 & n+1 \\ a^{n+1} & a^{n-1} & a^{1-n} & a^{-1-n} \\ (n+1)a^n & (n-1)a^{n-2} & (1-n)a^{-n} & (-1-n)a^{-2-n} \end{vmatrix} = 0. \tag{A5}$$

For $n = 1$ this condition is:

$$\begin{vmatrix} -(\alpha+4) & -\alpha & 4 & -(\alpha+4) \\ 4 & 0 & 0 & 4 \\ a^2 & 1 & \ln a & 1/a^2 \\ 2a & 0 & 1/a & -2/a^3 \end{vmatrix} = 0. \tag{A6}$$

These conditions yield the value $\alpha_c(n)$ of the load parameter α for which the total energy is invariant upon an infinitesimal change of the perturbation amplitude. This value depends on the circumferential mode n and on parameter a (see Eqs.18 and 17). Taking $\alpha = \alpha_c(n)$, one finds from Eqs.16 and 15 the expression of f_u up to a prefactor that is fixed so that $f_u(r_0) = \xi$. Then, from Eqs. (3.3) and (3.5) of [4], one deduces the expressions of f_Θ and f_q. Before writing the

analytic expressions of f_u, f_Θ and f_q, we first define four constants:

$$\begin{aligned}
A &= -\frac{a^{2n}\left(a^2-1\right)n^2+\left(a^{2n}+a^2\right)n-a^{2n+2}-a^2}{a^{2n}\left(2a^4-2\right)n-2a^{4n+2}+2a^2},\\
B &= \frac{a^{2n}\left(a^4-a^2\right)n^2+\left(a^{2n+4}+a^2\right)n+a^{2n+2}+a^2}{a^{2n}\left(2a^4-2\right)n-2a^{4n+2}+2a^2},\\
C &= \frac{a^{2n}\left(a^2-1\right)n^2+\left(-a^{4n+2}-a^{2n}\right)n-a^{4n+2}-a^{2n+2}}{a^{2n}\left(2a^4-2\right)n-2a^{4n+2}+2a^2},\\
D &= -\frac{a^{2n}\left(a^4-a^2\right)n^2+\left(-a^{4n+2}-a^{2n+4}\right)n+a^{4n+2}+a^{2n+2}}{a^{2n}\left(2a^4-2\right)n-2a^{4n+2}+2a^2}.
\end{aligned} \tag{A7}$$

The expressions of f_u, f_Θ and f_q are:

$$f_u = \left[A\left(\frac{r}{r_0}\right)^{n+1}+B\left(\frac{r}{r_0}\right)^{n-1}+C\left(\frac{r}{r_0}\right)^{1-n}+D\left(\frac{r}{r_0}\right)^{-n-1}\right]\xi, \tag{A8}$$

$$f_\Theta = -\left[A\frac{n+2}{n}\left(\frac{r}{r_0}\right)^{n}+B\left(\frac{r}{r_0}\right)^{n-2}+C\frac{2-n}{n}\left(\frac{r}{r_0}\right)^{-n}-D\left(\frac{r}{r_0}\right)^{-n-2}\right]\frac{\xi}{r_0}, \tag{A9}$$

$$\begin{aligned}
f_q = &\left[\left(-4A(n^2+n)-\alpha_c B\right)\left(\frac{r}{r_0}\right)^{n}+\left(4C(n-n^2)-\alpha_c D\right)\left(\frac{r}{r_0}\right)^{-n}\right.\\
&\left.-\alpha_c A\left(\frac{r}{r_0}\right)^{n+2}-\alpha_c C\left(\frac{r}{r_0}\right)^{2-n}\right]\frac{\xi}{r_0 n^2},
\end{aligned} \tag{A10}$$

with $\alpha=\alpha_c(n)$ (given by Eq.17). The previous expressions are for $n>1$. For $n=1$, we define:

$$A = \frac{a^2}{(2+2a^4)\ln a-a^4+1}, \tag{A11}$$

$$B = 1, \tag{A12}$$

$$C = -\frac{2+2a^4}{(2+2a^4)\ln a-a^4+1}, \tag{A13}$$

$$D = -\frac{a^2}{(2+2a^4)\ln a-a^4+1}, \tag{A14}$$

$$f_u = \left[\left(\frac{r_0}{r}\right)^2 D+\ln\left(\frac{r}{r_0}\right)C+B+\left(\frac{r}{r_0}\right)^2 A\right]\xi, \tag{A15}$$

$$f_\Theta = \left[\left(\frac{r_0}{r}\right)^3 D-\left(\frac{r_0}{r}\right)\left(1+\ln\left(\frac{r}{r_0}\right)\right)C-\left(\frac{r_0}{r}\right)B-3\left(\frac{r}{r_0}\right)A\right]\frac{\xi}{r_0}, \tag{A16}$$

$$f_q = \left[-\left(8\frac{r}{r_0}+\alpha_c\left(\frac{r}{r_0}\right)^3\right)A+\alpha_c\frac{r}{r_0}B+\left(\alpha_c\frac{r}{r_0}\ln\left(\frac{r}{r_0}\right)-2\frac{r_0}{r}\right)C+\alpha_c\frac{r_0}{r}D\right]\frac{\xi}{r_0} \tag{A17}$$

If one considers the limit $a\to 0$ with the circumferential wave number $n=1$, one obtains $(A,B,C,D)\to(0,1,0,0)$ hence $f_u=\xi$. Since $f_u(ar_0)=0$, the amplitude ξ of the mode with $n=1$ is fixed to 0 (for $a\to 0$, [4]).

Appendix B: Linear analysis including axial deformations

The main steps for the linear analysis introduced in Sec. III are detailed in this section.

We start from the sixth order differential equation, Eq.11, that was established previously in [4] in which the bifurcations in *homogeneous* spinning (solid) cylinders were investigated. The condition of zero traction at the lateral boundary ($r = r_0$) leads to three equations that were expressed in terms of f_u in [4], see Eqs. (A8) (A9) (A10) of [4]. The zero displacement condition at the inner interface of the elastic layer leads to three other boundary conditions, $f_u(ar_0) = 0$, $f_\Theta(ar_0) = 0$ and $f_z(ar_0) = 0$, that write, in terms of f_u (for $r = ar_0$):

$$f_u = 0, \tag{B1}$$

$$\frac{\mathrm{d}f_u}{\mathrm{d}r} = 0, \tag{B2}$$

$$r^3\frac{\mathrm{d}^5 f_u}{\mathrm{d}r^5} + 7r^2\frac{\mathrm{d}^4 f_u}{\mathrm{d}r^4} + r\left[\left(5-2n^2\right) - 2\left(kr\right)^2\right]\frac{\mathrm{d}^3 f_u}{\mathrm{d}r^3} - 6\left[1+2\left(kr\right)^2\right]\frac{\mathrm{d}^2 f_u}{\mathrm{d}r^2} = 0. \tag{B3}$$

In the following we calculate the general solution for Eq.11 for a given circumferential wave number n. This solution is defined up to 6 arbitrary constants. The solvability condition is fixed by the six boundary equations, and leads to a relation between α and a, defining the critical load $\alpha_c(n,k)$ at the linear instability threshold.

Although the physically admissible values of r are in the range $[ar_0, r_0]$, one can consider the mathematical solutions of Eq.11 in a the wider range of values of r, here in $[0, r_0]$. In order to find linearly independent solutions of Eq.11, we consider the mathematical behaviour of the solutions of this sixth order linear differential equation in the limit $r \to 0$. Let us first assume that $f_u(r) \sim r^p$ as $r \to 0$. Substituting this particular expression of f_u in Eq.11 and considering the limit $r \to 0$, the condition on exponent p is:

$$(n+p-3)(n-p-1)(n-p+1)(n-p+3)(n+p-1)(n+p+1) = 0. \tag{B4}$$

In the following, the linear solvability condition is derived for axisymmetric modes (circumferential wave number $n = 0$, Sec. B 1), and mixed modes with $n = 1$ (Sec. B 2), $n = 2$ (Sec. B 3) and $n = 3$ (Sec. B 4).

1. Axisymmetric modes

Here, we consider the deformations that are invariant by a continuous rotation about the axis of the cylinder, *i.e.* $n = 0$. The roots of Eq.B4, $p = -1, 1$ and 3 are double. We search accordingly six independent solutions of Eq.11, named $s_1(r)$, $s_2(r)$, $s_3(r)$, $s_4(r)$, $s_5(r)$ and $s_6(r)$ so that, for $r \to 0$, $s_1(r) \sim 1/r$, $s_2(r) \sim r$, $s_3(r) \sim r^3$, $s_4(r) \sim \ln r/r$, $s_5(r) \sim r \ln r$ and $s_6(r) \sim r^3 \ln r$. The general expression of the solutions of Eq.11 are therefore sought as:

$$s_i(r) = \frac{a_{-1}}{kr} + \frac{b_{-1}\ln(kr)}{kr} + \sum_{m=0}^{\infty} \left(a_m + b_m \ln(kr)\right)(kr)^m. \tag{B5}$$

The substitution of this expression in Eq.11 yields the conditions on the sequences $(a_m)_{m\geq -1}$ and $(b_m)_{m\geq -1}$:

$$b_{-1} - 12b_1 + 192b_3 - 2304b_5 = 0, \tag{B6}$$

$$a_{-1} - 12a_1 + 192a_3 - 2304a_5 - 12b_1 + 288b_3 - 4224b_5 = 0, \tag{B7}$$

$$b_{m-6} - 3(m-3)^2 b_{m-4} + 3(m-3)^2(m-1)^2 b_{m-2} - (m-3)^2(m-1)^2(m+1)^2 b_m = 0 \quad \forall m \geq 6 \tag{B8}$$

$$a_{m-6} - 3(m-3)^2 a_{m-4} + 3(m-3)^2(m-1)^2 a_{m-2} - (m-3)^2(m^2-1)^2 a_m$$
$$-6(m-3)b_{m-4} + 12(m-1)(m-2)(m-3)b_{n-2} + 2(m-3)(m^2-1)(1+6m-3m^2)b_m = 0$$
$$\forall m \geq 6.$$

Moreover, a_m and b_m are equal to 0 if n is an even number. Eqs.B6 and B7 involve 8 unknowns (a_{-1}, a_1, a_3, a_5, b_{-1}, b_1, b_3, b_5), leaving 6 free unknown that are chosen accordingly with the prescribed behaviour of the functions s_i for $r \to 0$, leading to the following sequences:

$a_{-1} = 1$, $a_1 = a_3 = 0$, $b_{-1} = b_1 = b_3 = 0$ for $s_1(r)$,

$a_{-1} = 0$, $a_1 = 1$, $a_3 = 0$, $b_{-1} = b_1 = b_3 = 0$ for $s_2(r)$,

$a_{-1} = a_1 = 0$, $a_3 = 1$, $b_{-1} = b_1 = b_3 = 0$ for $s_3(r)$,

$a_{-1} = 1$, $a_1 = a_3 = 0$, $b_{-1} = 1$, $b_1 = b_3 = 0$ for $s_4(r)$,

$a_{-1} = 0$, $a_1 = 1$, $a_3 = 0$, $b_{-1} = 0$, $b_1 = 1$, $b_3 = 0$ for $s_5(r)$,

$a_{-1} = a_1 = 0$, $a_3 = 1$, $b_{-1} = b_1 = 0$, $b_3 = 1$ for $s_6(r)$.

Writing $f_u(r)$ as:

$$f_u(r) = \sum_{i=1}^{6} A_i s_i(r), \tag{B9}$$

and substituting this expression of $f_u(r)$ in the boundary equations, one obtains a homogeneous linear system of 6 equations with 6 unknowns. The solvability condition implies that the matrix

of the system is singular, hence the equation defining the threshold value of α_c as a function of k that is solved numerically and plotted in Fig.3.

2. Asymmetric mode with the circumferential wave number $n = 1$

We now focus on mixed modes with the circumferential wave number $n = 1$. The roots of Eq.B4 are $p = -2, 0, 2, 4$ (2 and 0 are double roots). Then we search six independent solutions of Eq.11 so that, for $r \to 0$, $s_1(r) \sim 1/r^2$, $s_2 \sim 1$, $s_3(r) \sim \ln r$, $s_4(r) \sim r^2$, $s_5 \sim r^2 \ln r$, $s_6 \sim r^4$, in the form of the series expansion:

$$s_i(r) = \frac{a_{-2}}{r^2} + \sum_{m=0}^{\infty} \left(a_m + b_m \ln(kr)\right) (kr)^m. \tag{B10}$$

The substitution of this expression in Eq.11 yields the condition on the sequences $(a_m)_{m\geq -2}$ and $(b_m)_{m\geq 0}$:

$$a_{-2} - 6b_0 + 48b_2 - 384b_4 = 0, \tag{B11}$$

$$b_{m-6} - 3(m-4)(m-2)b_{m-4} + 3(m-4)(m-2)^2 m b_{m-2} - (m-4)(m-2)^2 m^2 (2+m) b_m = 0 \; \forall m \geq 6, \tag{B12}$$

$$\begin{aligned} &a_{m-6} - 3(m-4)(m-2)a_{m-4} + 3(m-4)(m-2)^2 m a_{m-2} \\ &-(m-4)(m-2)^2 m^2 (m+2) a_m - 6(m-3)b_{m-4} + 12(m-2)(m^2-4m+2)b_{m-2} \\ &-2(m-2)(m-1)m(-16-6m+3m^2)b_m = 0 \; \forall m \geq 6. \end{aligned} \tag{B13}$$

Moreover, a_m and b_m are equal to 0 for n odd number. Accordingly with the prescribed behaviour of the functions s_i for $r \to 0$, we take the following sequences :

$a_{-2} = 1$, $a_0 = a_2 = a_4 = b_0 = b_2 = 0$ for $s_1(r)$,

$a_{-2} = 0$, $a_0 = 1$, $a_2 = a_4 = b_0 = b_2 = 0$ for $s_2(r)$,

$a_{-2} = a_0 = a_2 = a_4 = 0$, $b_0 = 1$, $b_2 = 0$ for $s_3(r)$,

$a_{-2} = a_0 = 0$, $a_2 = 1$, $a_4 = b_0 = b_2 = 0$ for $s_4(r)$,

$a_{-2} = a_0 = a_2 = a_4 = b_0 = 0$, $b_2 = 1$ for $s_5(r)$,

$a_{-2} = a_0 = a_2 = 0$, $a_4 = 1$, $b_0 = b_2 = 0$ for $s_6(r)$.

Following the same procedure as in Sec. B 1, one then obtains the threshold value α_c as a function of k for $n = 1$ (See Fig.3).

3. Asymmetric mode with the circumferential wave number $n = 2$

We now deal with mixed modes with the circumferential wave number $n = 2$. The roots of Eq.B4 are $p = -3, -1, 1$ (double root), 3 and 5. Then we search six independent solutions of Eq.11 so that, for $r \to 0$, $s_1(r) \sim 1/r^3$, $s_2(r) \sim 1/r$, $s_3(r) \sim r$, $s_4 \sim r \ln r$, $s_5 \sim r^3$ and $s_6 \sim r^5$, in the form of the series expansion:

$$s_i(r) = \frac{a_{-3}}{(kr)^3} + \frac{a_{-1}}{kr} + \sum_{m=0}^{\infty} \left(a_m + b_m \ln(kr)\right) (kr)^m. \tag{B14}$$

The substitution of this expression in Eq.11 yields the condition on the sequences $(a_m)_{m\geq -3}$ and $(b_m)_{m\geq 0}$:

$$-48b_1 + 192b_3 + 12a_{-1} + a_{-3} = 0, \tag{B15}$$

$$-12b_1 + 144b_3 - 1536b_5 + a_{-1} = 0, \tag{B16}$$

$$\begin{aligned} b_{m-6} - 3(m-5)(m-1)b_{m-4} + 3(m-5)(m-3)(m^2-1)b_{m-2} \\ -b_m(m-5)(m^2-9)(m-1)^2(m+1) = 0 \quad \forall m \geq 6, \end{aligned} \tag{B17}$$

$$\begin{aligned} a_{m-6} - 3(m-5)(m-1)a_{m-4} + 3(m-5)(m-3)(m^2-1)a_{m-2} \\ -(m-5)(m^2-9)(m-1)^2(m+1)a_n \\ -6(m-3)b_{m-4} + 12(m-2)(m^2-4m-1)b_{m-2} \\ -2(m-1)(27+68m-22m^2-12m^3+3m^4)b_m = 0 \quad \forall n \geq 6. \end{aligned} \tag{B18}$$

Moreover, a_m and b_m are equal to 0 for n even number. Accordingly with the prescribed behaviour of the functions s_i for $r \to 0$, we take the following sequences :

$a_{-3} = 1$, $a_{-1} = a_1 = a_3 = a_5 = b_1 = 0$ for $s_1(r)$,

$a_{-3} = 0$, $a_{-1} = 1$, $a_1 = a_3 = a_5 = 0 = b_1 = 0$ for $s_2(r)$,

$a_{-3} = 0 = a_{-1} = 0$, $a_1 = 1$, $a_3 = a_5 = b_1 = 0$ for $s_3(r)$,

$a_{-3} = a_{-1} = a_1 = a_3 = a_5 = 0$, $b_1 = 1$ for $s_4(r)$,

$a_{-3} = a_{-1} = a_1 = 0$, $a_3 = 1$, $a_5 = b_1 = 0$ for $s_5(r)$,

$a_{-3} = a_{-1} = a_1 = a_3 = 0$, $a_5 = 1$, $b_1 = 0$ for $s_6(r)$.

Following the same procedure as in Sec. B 1, one then obtains the threshold value α_c as a function of k for $n = 2$ (See Fig.3).

4. Asymmetric mode with the circumferential wave number $n = 3$

For $n = 3$, the roots of Eq.B4 are $p = -4, -2, 0, 2, 4$ and 6. Then, we take $s_1(r) \sim 1/r^4$, $s_2(r) \sim 1/r^2$, $s_3(r) \sim 1$, $s_4 \sim r^2$, $s_5 \sim r^4$ and $s_6 \sim r^6$ for $r \to 0$. Function $s_i(r)$ are sought as:

$$s_i(r) = \frac{a_{-4}}{(kr)^4} + \frac{a_{-2}}{(kr)^2} + \sum_{m=0}^{\infty} \left(a_m + b_m \ln(kr)\right) (kr)^m, \tag{B19}$$

leading to the conditions:

$$24a_0 - 144b_2 + 768b_4 + a_{-2} = 0, \tag{B20}$$

$$192a_0 - 384b_2 + 24a_{-2} + a_{-4} = 0, \tag{B21}$$

$$\begin{aligned} &b_{m-6} - 3(m-6)mb_{m-4} + 3(m-6)(m-4)m(m+2)b_{m-2} \\ &-(m-6)(m-4)(m-2)m(m+2)(m+4)b_m = 0 \quad \forall m \geq 6, \end{aligned} \tag{B22}$$

$$\begin{aligned} a_{m-6} - 3(m-6)ma_{m-4} + 3(m-6)(m-4)m(m+2)a_{m-2} \\ -(m-6)(m^2-16)(m^2-4)ma_m \\ -6(m-3)b_{m-4} + 12(m-2)(m^2-4m-6)b_{m-2} \\ -2(m-1)(192+128m-52m^2-12m^3+3m^4)b_m = 0 \quad \forall m \geq 6. \end{aligned} \tag{B23}$$

Moreover, a_m and b_m are equal to 0 for n even number. Accordingly with the prescribed behaviour of the functions s_i for $r \to 0$, we take the following sequences :

$a_0 = 1$, $a_2 = a_4 = a_6 = b_2 = b_4 = 0$ for $s_1(r)$,

$a_{-4} = 0$, $a_{-2} = 1$, $b_4 = a_2 = a_4 = a_6 = 0$ for $s_2(r)$,

$a_{-4} = a_{-2} = 0$, $a_0 = 1$, $a_2 = a_4 = a_6 = 0$ for $s_3(r)$,

$a_{-4} = a_{-2} = a_0 = 0$, $a_2 = 1$, $a_4 = a_6 = 0$ for $s_4(r)$,

$a_{-4} = a_{-2} = a_0 = 0 = a_2 = 1$, $a_4 = 1$, $a_6 = 0$ for $s_5(r)$,

$a_{-4} = a_{-2} = a_0 = a_2 = a_4 = 0$, $a_6 = 1$ for $s_6(r)$.

Following the same procedure as in Sec. B 1, one then obtains the threshold value α_c as a function of k for $n = 3$ (See Fig.3).

The same analyze, done for circumferential wave numbers $n \geq 4$, qualitatively leads to the same structure for $\alpha_c(n, k)$.

Appendix C: Calculation of the displacement field at order 2 in the weakly non linear analysis

The key steps in the calculation of the second order solution in the post buckling expansion are introduced in this appendix.

For the neo-Hookean constitutive law we consider, the strain energy density function is $W = \frac{1}{2}(I_1 - 3)$. The strong form of the equilibrium condition Eq.5 is deduced from Eqs. (2.5)-(2.9) of [4]. It is:

$$\frac{R}{r}\left(R_{,r}\Theta_{,\theta} - R_{,\theta}\Theta_{,r}\right) = 1, \tag{C1}$$

$$-\left(rR_{,r}\right)_{,r} - \frac{R_{,\theta\theta}}{r} + rR\left(\Theta_{,r}\right)^2 + \frac{R}{r}\left(\Theta_{,\theta}\right)^2 - Rq_{,r}\Theta_{,\theta} + Rq_{,\theta}\Theta_{,r} = \alpha\frac{rR}{r_0^2}, \tag{C2}$$

$$\left(rR^2\Theta_{,r}\right)_{,r} + \frac{1}{r}\left(R^2\Theta_{,\theta}\right)_{,\theta} + Rq_{,\theta}R_{,r} - Rq_{,r}R_{,\theta} = 0, \tag{C3}$$

$$rR_{,r} + qR\Theta_{,\theta} = 0 \text{ at } r = r_0, \tag{C4}$$

$$rR\Theta_{,r} - qR_{\theta} = 0 \text{ at } r = r_0, \tag{C5}$$

$$R = r \text{ at } r = ar_0, \tag{C6}$$

$$\Theta = \theta \text{ at } r = ar_0, \tag{C7}$$

where a subscript comma denotes a partial derivative. Eq.C1 is the incompressibility constraint, Eqs.C2 and C3 are the equilibrium conditions in the radial and circumferential directions respectively, Eqs.C4 and C5 are the zero traction condition at the lateral boundary $r = r_0$, and Eqs.C6 and C7 are the zero displacement condition at the rigid inner rod.

The expansions defined in Eqs.19 and 20 are first put in Eqs.C1-C7:

$$\begin{aligned}
\alpha &= \alpha_c + \varepsilon^2\alpha_2, \\
R &= r + \varepsilon u_1 + \varepsilon^2 u_2, \\
\Theta &= \theta + \varepsilon\Theta_1 + \varepsilon^2\Theta_2, \\
q &= q_0 + \varepsilon q_1 + \varepsilon^2 q_2.
\end{aligned}$$

q_0, as defined by Eq.9, contains known contributions at order ε^0 and at order ε^2. u_1, Θ_1 and q_1 have been calculated up to the amplitude ξ in the linear analysis (Appendix A). u_2, Θ_2 and q_2 are defined by Eqs.25-27 through the unknown functions g_u, g_Θ, g_q, $\bar{g}_u$, $\bar{g}_\Theta$ and $\bar{g}_q$. The goal is here to find the expressions of these 6 functions for given a, n, α_2 and ξ.

Eqs.C1-C7 at order ε^2 yield a set of 7 equations. Each one can be separated in two parts : one is independent of θ and involves $\bar{g}_u$, $\bar{g}_\Theta$ and $\bar{g}_q$. The other part depends on θ like $\cos(4n\theta)$ or $\sin(4n\theta)$ and involves g_u, g_Θ and g_q. At the end, one obtains 14 differential equations:

- 3 coupled linear differential equations in the bulk for g_u, g_q and g_Θ with 4 boundary conditions (at $r = r_0$ and $r = ar_0$);
- 3 coupled linear differential equations in the bulk for $\bar{g}_u$, $\bar{g}_q$ and $\bar{g}_\Theta$ with 4 boundary conditions (at $r = r_0$ and $r = ar_0$);

Combining the θ dependent terms of order ε^2 arising from Eqs.C2, C3 and C1, one obtains a fourth order linear differential equation for g_u:

$$r^3\frac{\mathrm{d}^4 g_u}{\mathrm{d}r^4} + 6r^2\frac{\mathrm{d}^3 g_u}{\mathrm{d}r^3} - (8n^2-5)r\frac{\mathrm{d}^2 g_u}{\mathrm{d}r^2} - (8n^2+1)\frac{\mathrm{d}g_u}{\mathrm{d}r} + (4n^2-1)^2\frac{g_u}{r} = -\left(\frac{\xi}{r_0}\right)^2 h_1, \quad \text{(C8)}$$

where h_1 is a function of r/r_0, n and a. The complete expression of h_1 is given in [28]. The solutions of Eq.C8 can be written as:

$$g_u(r) = A_2 r^{-(2n+1)} + B_2 r^{-(2n-1)} + C_2 r^{2n-1} + D_2 r^{2n+1} + \left(\frac{\xi}{r_0}\right)^2 \gamma(r), \quad \text{(C9)}$$

with

$$\begin{aligned} \gamma(r) &= \ln\frac{r}{r_0}\left(k_0\frac{r}{r_0} + k_1\frac{r_0}{r} + k_2\left(\frac{r_0}{r}\right)^3 + k_4\frac{r_0}{r}\ln\frac{r}{r_0}\right) + k_3\left(\frac{r_0}{r}\right)^5 \text{ for } n = 1, \\ \gamma(r) &= k_0 r/r0 + k_1(r/r_0)^{2n-3} + \frac{k_2}{(r/r_0)^3} + k_3(r/r_0)^{-(2n+3)} + \frac{k_4}{(r/r_0)} \text{ for } n > 1. \end{aligned} \quad \text{(C10)}$$

A_2, B_2, C_2 and D_2 are four constants and k_0, k_1, k_2, k_3 and k_4 depend on a and n. Their complete expressions are written in [28]. From Eqs.C4, C5, C1, and C3 at order ε^2, one obtains the boundary conditions at $r = r_0$ expressed in terms of g_u:

$$r_0^3\frac{\mathrm{d}^3 g_u}{\mathrm{d}r^3}(r_0) + 4r_0^2\frac{\mathrm{d}^2 g_u}{\mathrm{d}r^2}(r_0) - (12n^2-1)r_0\frac{\mathrm{d}g_u}{\mathrm{d}r}(r_0) + h_2 g_u(r_0) = -\frac{\xi^2}{r_0}h_3, \quad \text{(C11)}$$

$$r_0^2\frac{\mathrm{d}^2 g_u}{\mathrm{d}r^2}(r_0) + r_0\frac{\mathrm{d}g_u}{\mathrm{d}r}(r_0) + (4n^2-1)g_u(r_0) = -\frac{\xi^2}{2r_0}h_4. \quad \text{(C12)}$$

h_2, h_3 and h_4 are three functions of a and n, whose detailed expressions are given in [28]. The two remaining boundary conditions to be taken into account in order to determine the constants A, B, C and D in Eq.C9 are:

$$g_u(ar_0) = 0, \quad \text{(C13)}$$

$$g_\Theta(ar_0) = 0. \quad \text{(C14)}$$

Eq.C14 is expressed with g_Θ which can be written in terms of g_u using Eq.C1.
Inserting Eq.C10 in the four boundary equations, Eqs.C11-C14, one obtains a system of four equations with four unknowns, A_2, B_2, C_2 and D_2, that are determined as a function of a and n, hence the complete analytical expression for $g_u(r)$.

g_Θ and g_q are obtained from Eqs.C1 and C3 respectively, by inserting in these equations the previous expression of g_u.

Taking now the terms independent of θ in the second order term of Eq.C1, one obtains a first order differential equation for $\bar{g}_u$:

$$r\frac{\mathrm{d}\bar{g}_u}{\mathrm{d}r} + \bar{g}_u = \frac{r_0^2\xi^2}{r^3}h_7, \tag{C15}$$

with h_7 a function of a, n and r/r_0 whose expression is given in [28]. This first order linear differential equation can be solved using the variation of parameters method up to a constant, which is fixed with the θ-independent part of boundary condition Eq.C6 at order ε^2:

$$\bar{g}_u(ar_0) = 0. \tag{C16}$$

The expression of $\bar{g}_u$ being now known, the first derivative of $\bar{q}_q$, $\mathrm{d}\bar{q}_q/\mathrm{d}r$, can be calculated from the θ-independent part of Eq.C2 at order ε^2 which is:

$$r\frac{\mathrm{d}^2\bar{g}_u}{\mathrm{d}r^2} + \frac{\mathrm{d}\bar{g}_u}{\mathrm{d}r} + r\frac{\mathrm{d}\bar{g}_q}{\mathrm{d}r} - \frac{\bar{g}_u}{r} = -\frac{\xi^2}{r_0^2}h_5. \tag{C17}$$

h_5 is a function of a, n and r/r_0 whose expression is given in [28]. The expression of $\bar{g}_q$ is obtained by integration of $\mathrm{d}\bar{q}_q/\mathrm{d}r$ with the boundary condition Eq.C4 which is:

$$r_0\frac{\mathrm{d}\bar{g}_u}{\mathrm{d}r}(r_0) - \bar{g}_u(r_0) + r_0\bar{g}_q(r_0) = -h_6, \tag{C18}$$

where h_6 is a function of a and n, whose expression is given in [28].

The θ-independent part of Eq.C3 yields the first order linear homogeneous differential equation for $\mathrm{d}\bar{q}_\Theta/\mathrm{d}r$:

$$r^3\frac{\mathrm{d}^2\bar{g}_\Theta}{\mathrm{d}r^2} + 3r^2\frac{\mathrm{d}\bar{g}_\Theta}{\mathrm{d}r} = 0. \tag{C19}$$

With C5 and C6, which write respectively at order ε^2:

$$\frac{\mathrm{d}\bar{g}_\Theta}{\mathrm{d}r}(r_0) = 0, \tag{C20}$$

and

$$\bar{g}_\Theta(ar_0) = 0, \tag{C21}$$

one deduces that $\bar{g}_\Theta = 0$.

Appendix D: List of symbols assigned to specific load parameters and relative inner radii

The symbols defining special values of the load parameter α and special values of the relative inner radius a used in Sections III, IV and V are summarized below. n is the order of the rotational symmetry of the buckled configuration, and n_{first} is the value of n of the first mode that is linearly unstable when α is gradually increased from 0. n_{first} depends on a.

Symbol	Description
a_n^{linear}	value of a at the crossover from $n_{\text{first}} = n-1$ to $n_{\text{first}} = n$
a_n^-	lowest value of a so that mode n is sub-critical
a_n^+	lowest value of a for a crossover from sub-critical to super-critical (for fixed mode n)
$\alpha_c(n)$	critical load at the linear instability threshold. $\alpha_c(n)$ also depends on a
$\alpha^*(n_{\text{mesh}})$	critical load at the linear instability threshold calculated with finite elements with the linear mesh density n_{mesh}. $\alpha^*(n_{\text{mesh}})$ also depends on a and n
$\alpha_m(n)$	lowest admissible load for a buckled configuration with a rotational symmetry of order n. $\alpha_m(n)$ also depends on a
α_m	lowest admissible load for a buckled configuration, whatever the rotational order. α_m depends on a